Nuclear Lattice Effective Field Theory

Dean Lee
Facility for Rare Isotope Beams
Michigan State University
Nuclear Lattice EFT Collaboration

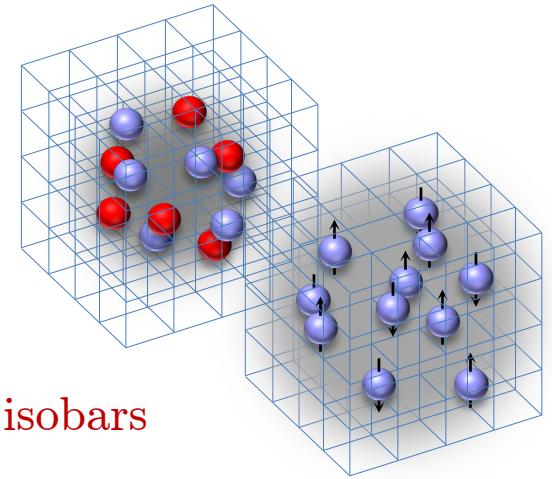

EMMI Rapid Reaction Task Force
Nuclear physics confronts relativistic collisions of isobars
Part 1: May 30 – June 3, 2022
University of Heidelberg

FRIB
MICHIGAN STATE UNIVERSITY
NUCLEI Nuclear Computational Low-Energy Initiative A SciDAC-4 Project
JÜLICH FORSCHUNGSZENTRUM
OAK RIDGE National Laboratory | LEADERSHIP COMPUTING FACILITY

Outline

Lattice effective field theory

Hidden spin-isospin exchange symmetry

Essential elements for nuclear binding

^{16}O ^{16}O collisions at RHIC and LHC energies

Nuclear thermodynamics

Structure and spectrum of ^{12}C

Wave function matching

Summary

Lattice effective field theory

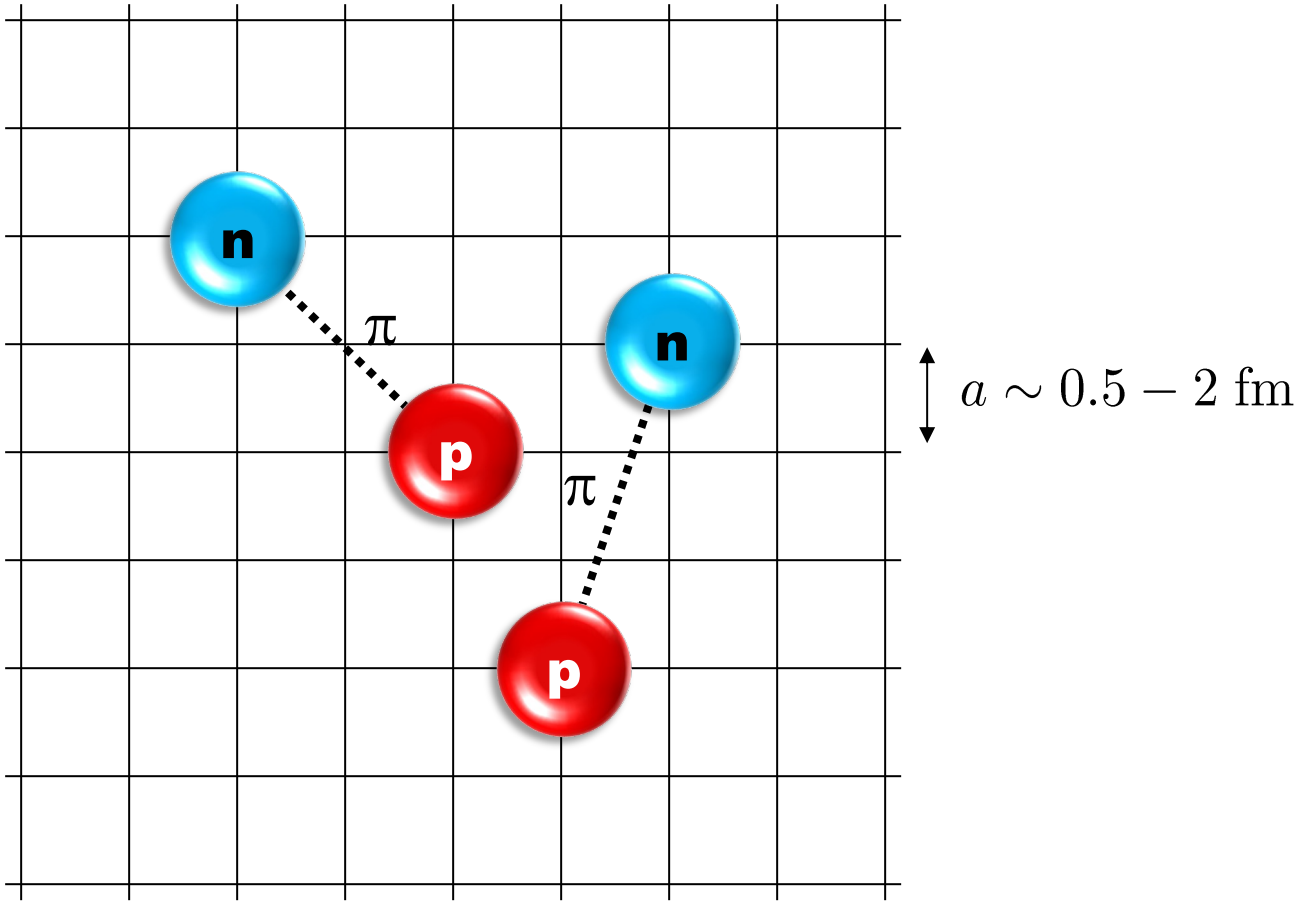

[D.L, Prog. Part. Nucl. Phys. 63 117-154 (2009)]

[Lähde, Meißner, Nuclear Lattice Effective Field Theory (2019), Springer]

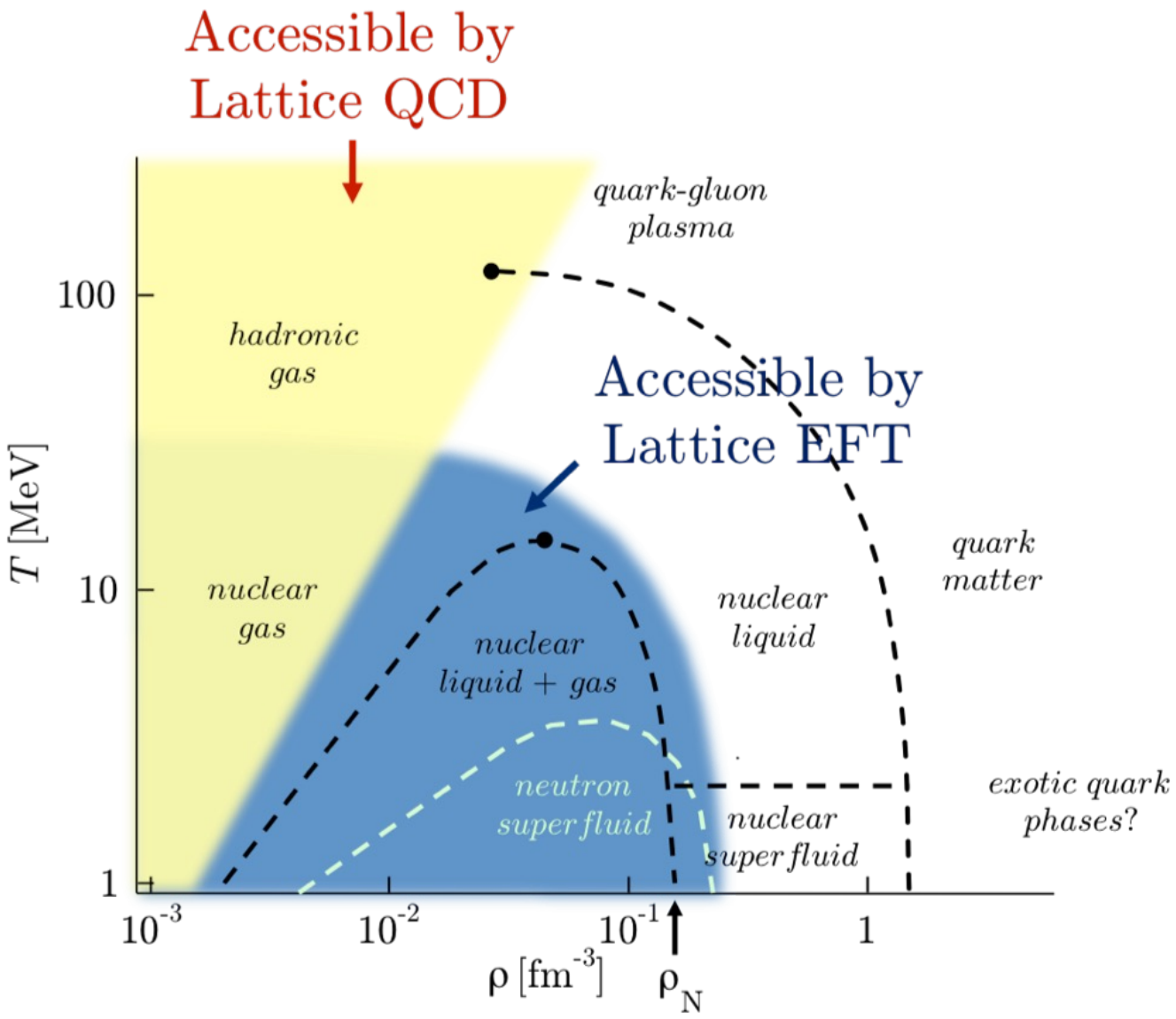
Accessible by
Lattice QCD
quark-gluon
plasma
hadronic
gas
Accessible by
Lattice EFT
quark
matter
nuclear
gas
nuclear
liquid
nuclear
liquid + gas
neutron
superfluid
nuclear
superfluid
exotic quark
phases?
100
10
1
T [MeV]
10^-3
10^-2
10^-1
1
ρ [fm^-3]
ρ_N

Chiral effective field theory

Construct the effective potential order by order

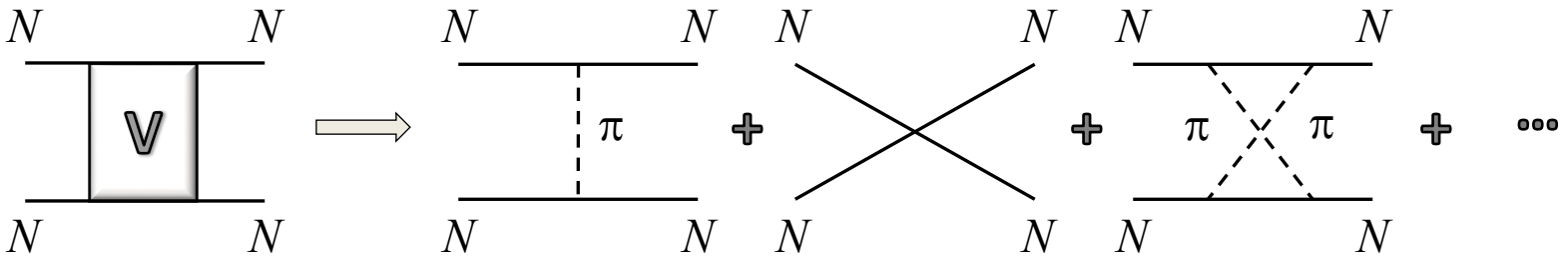

V^{OPEP} Contact interactions V^{TPEP}

Leading order (LO) Next-to-leading order (NLO)

$a = 1.315\,\mathrm{fm}$

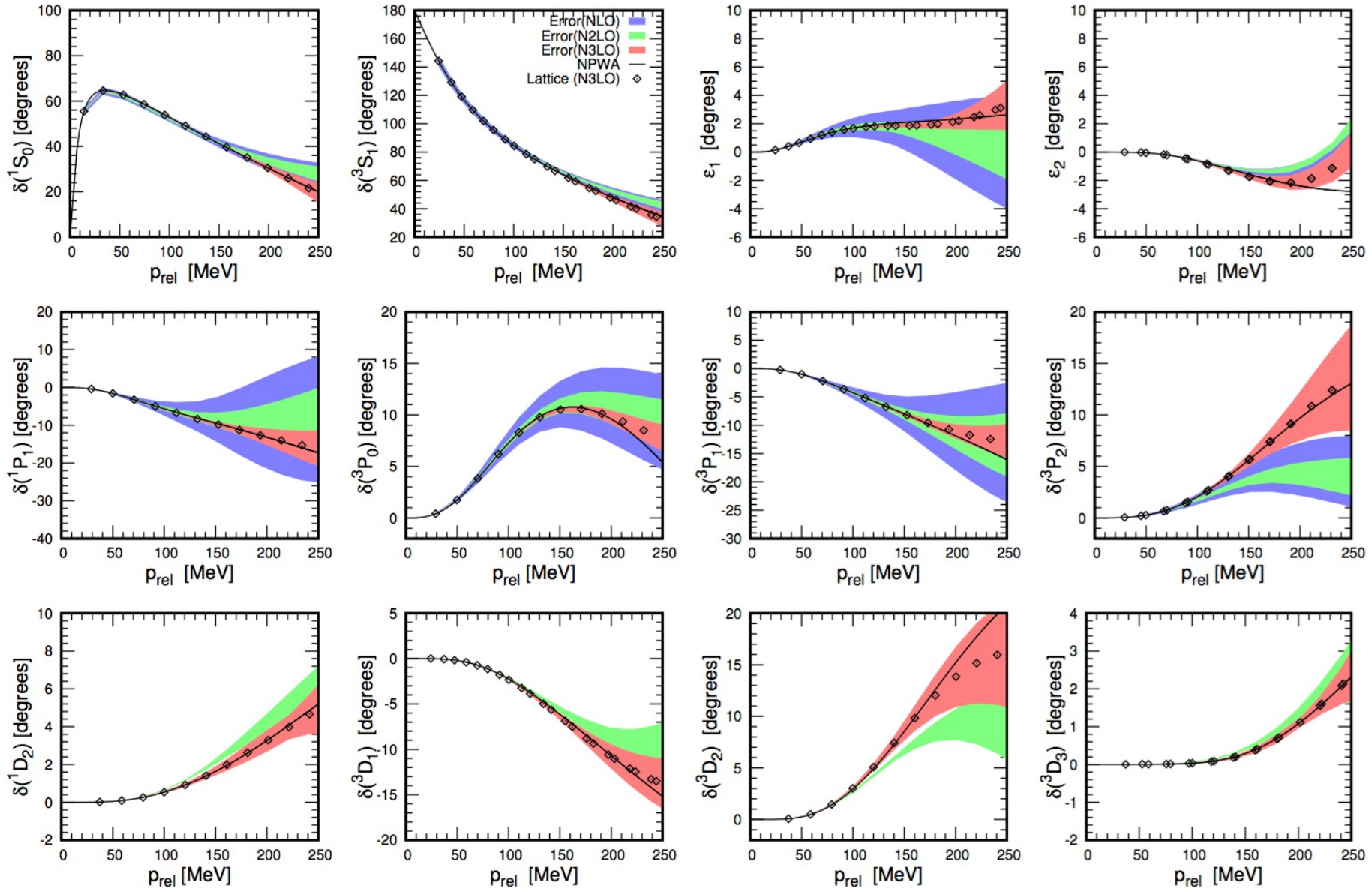

[Li, Elhatisari, Epelbaum, D.L., Lu, Meißner, PRC 98, 044002 (2018)]

$a = 0.987\,\mathrm{fm}$

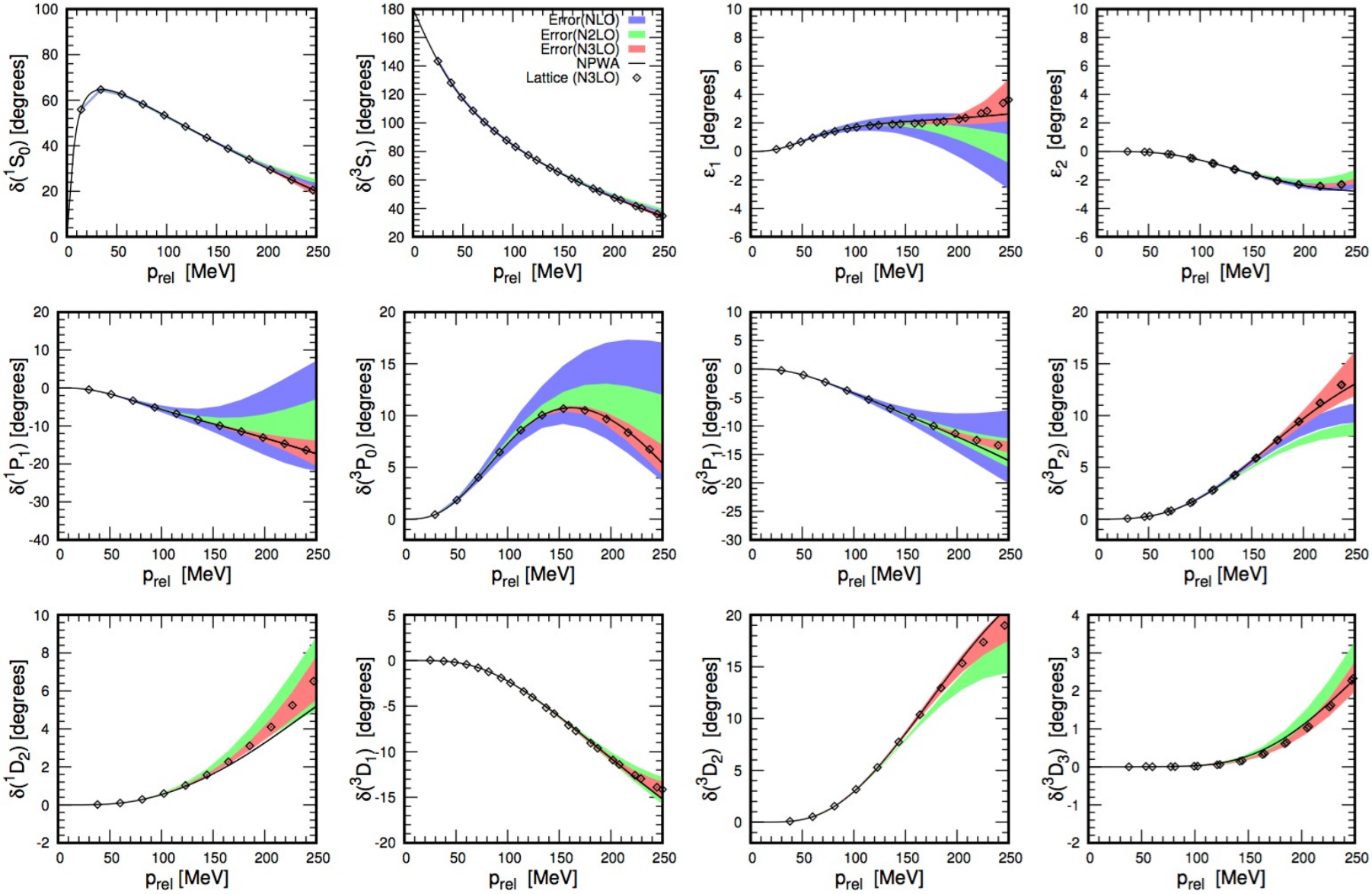

Euclidean time projection

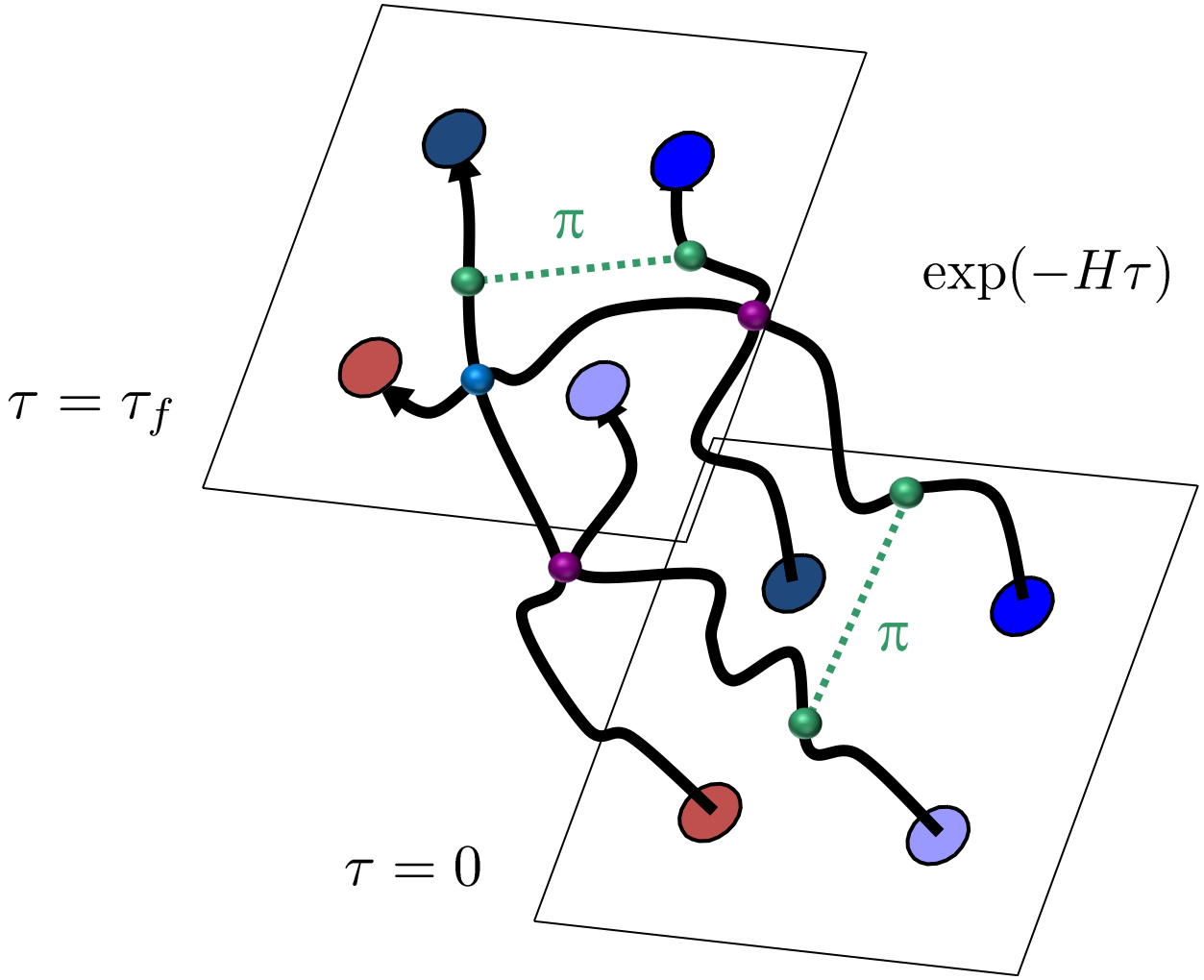

Auxiliary field method

We can write exponentials of the interaction using a Gaussian integral identity

$$\exp\left[-\frac{C}{2}(N^\dagger N)^2\right] \qquad \times \quad (N^\dagger N)^2$$

$$= \sqrt{\frac{1}{2\pi}}\int_{-\infty}^{\infty} ds \exp\left[-\frac{1}{2}s^2 + \sqrt{-C}\, s(N^\dagger N)\right] \qquad \rangle \bullet \; sN^\dagger N$$

We remove the interaction between nucleons and replace it with the interactions of each nucleon with a background field.

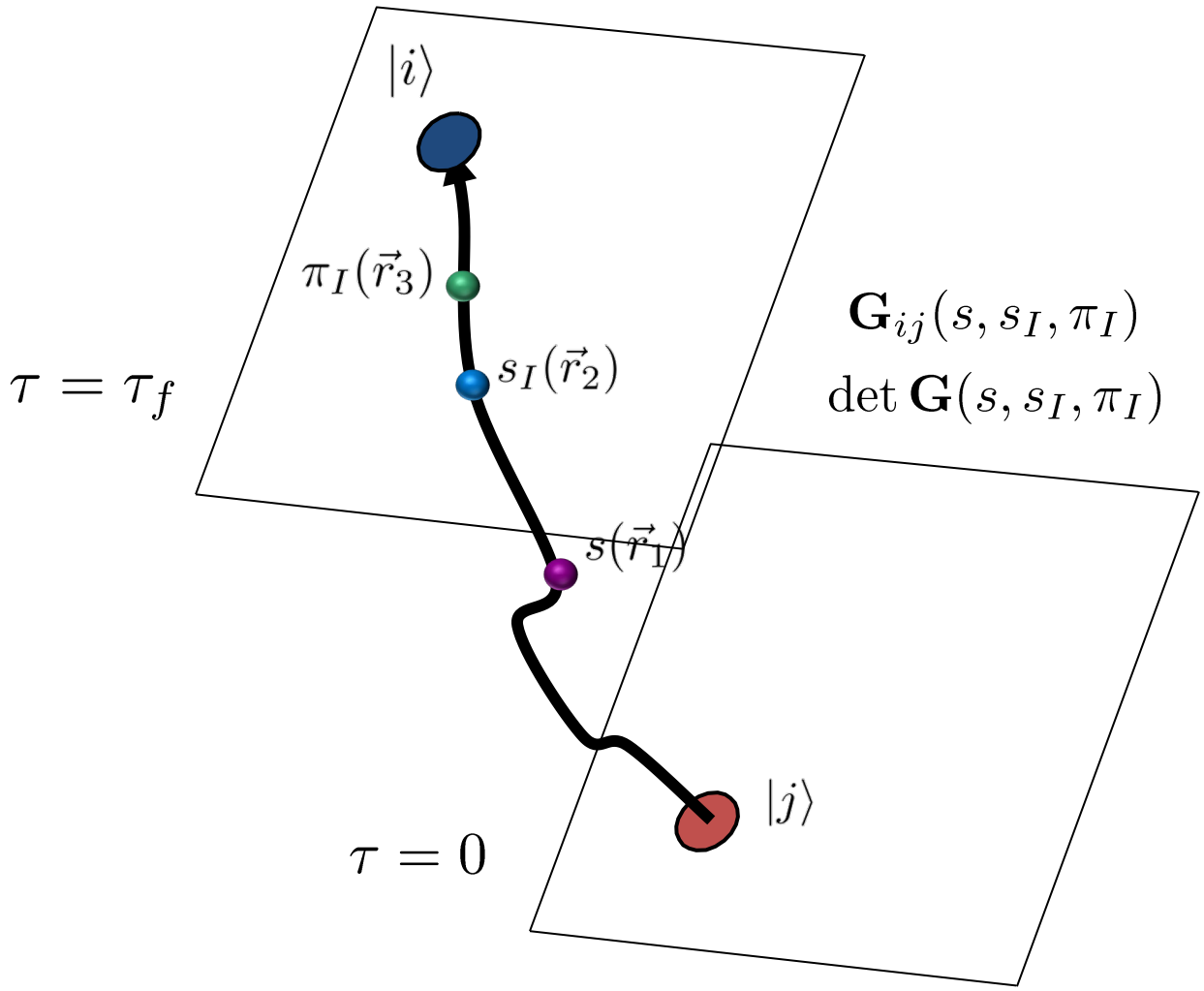
$|i\rangle$
$\pi_I(\vec{r}_3)$
$s_I(\vec{r}_2)$
$s(\vec{r}_1)$
$|j\rangle$
$\tau = \tau_f$
$\tau = 0$
$\mathbf{G}_{ij}(s, s_I, \pi_I)$
$\det \mathbf{G}(s, s_I, \pi_I)$

Hidden spin-isospin exchange symmetry

Kaplan, Savage, PLB 365, 244 (1996)

Kaplan, Manohar, PRC 56, 76 (1997)

Calle Gordon, Arriola, PRC 80, 014002 (2009)

$$V^{2N}_{\text{large}-N_c} = V_C + \vec{\sigma}_1 \cdot \vec{\sigma}_2 \vec{\tau}_1 \cdot \vec{\tau}_2 W_S + (3\hat{r} \cdot \vec{\sigma}_1 \hat{r} \cdot \vec{\sigma}_2 - \vec{\sigma}_1 \cdot \vec{\sigma}_2)\vec{\tau}_1 \cdot \vec{\tau}_2 W_T$$

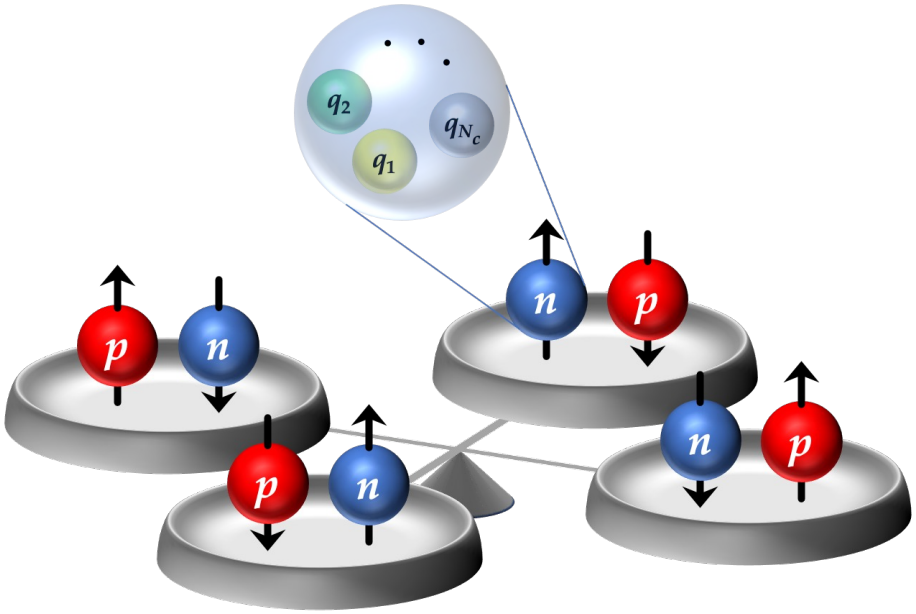

[D.L., Bogner, Brown, Elhatisari, Epelbaum, Hergert, Hjorth-Jensen, Krebs, Li, Lu, Meißner, PRL 127, 062501 (2021)]

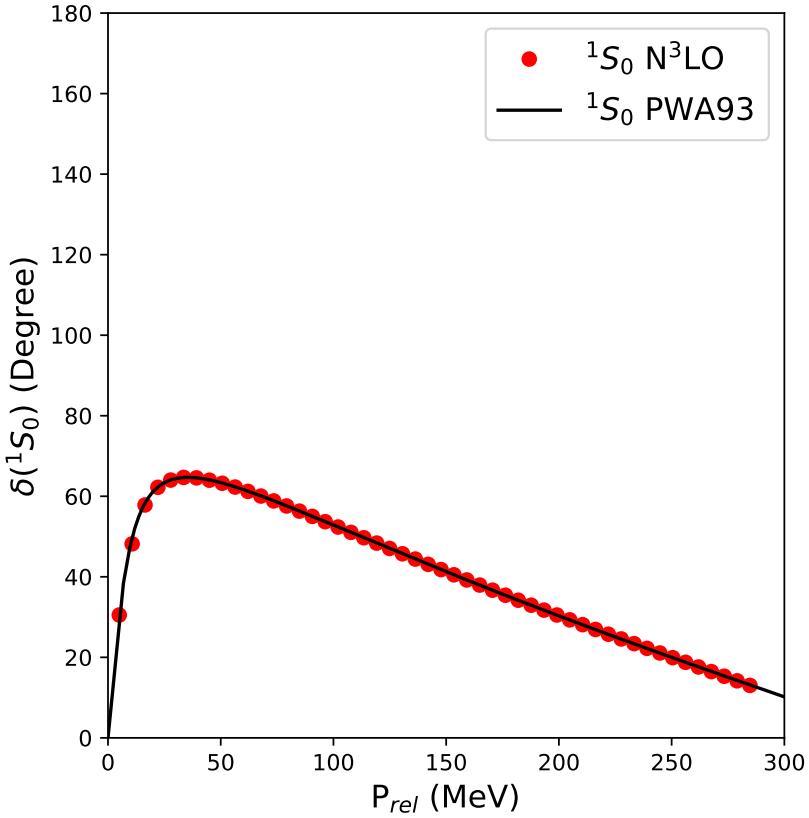
180
160
140
120
100
80
60
40
20
0
0
50
100
150
200
250
300
$\delta(^1S_0)$ (Degree)
P_{rel} (MeV)
$^1S_0$ N^{3}LO
$^1S_0$ PWA93

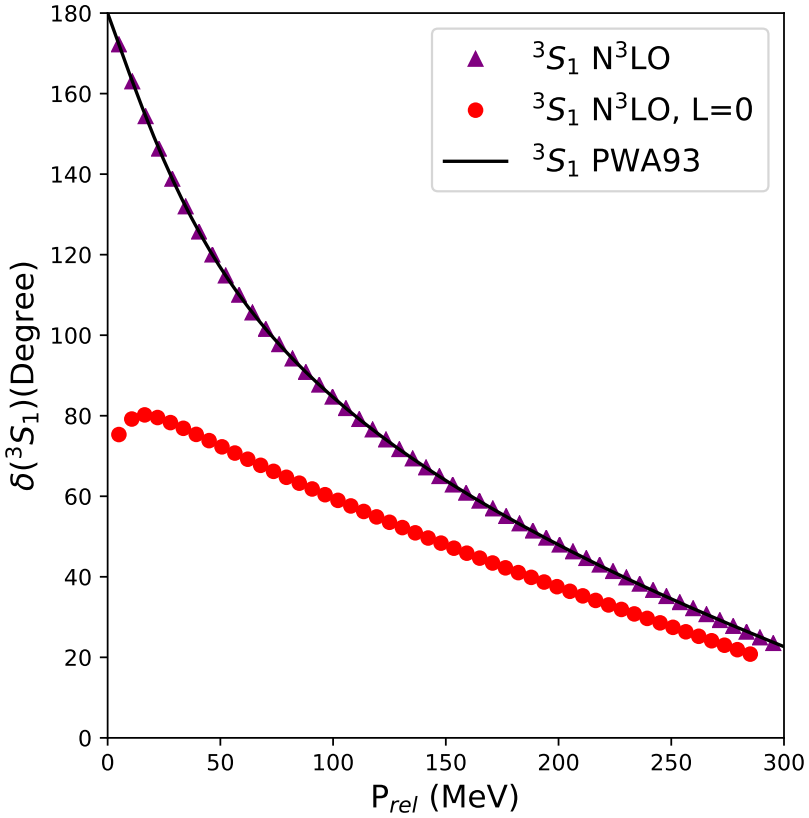
180
160
140
120
100
80
60
40
20
0
0
50
100
150
200
250
300
$\delta(^3S_1)$(Degree)
P_{rel} (MeV)
$^3S_1$ N^{3}LO
$^3S_1$ N^{3}LO, L=0
$^3S_1$ PWA93

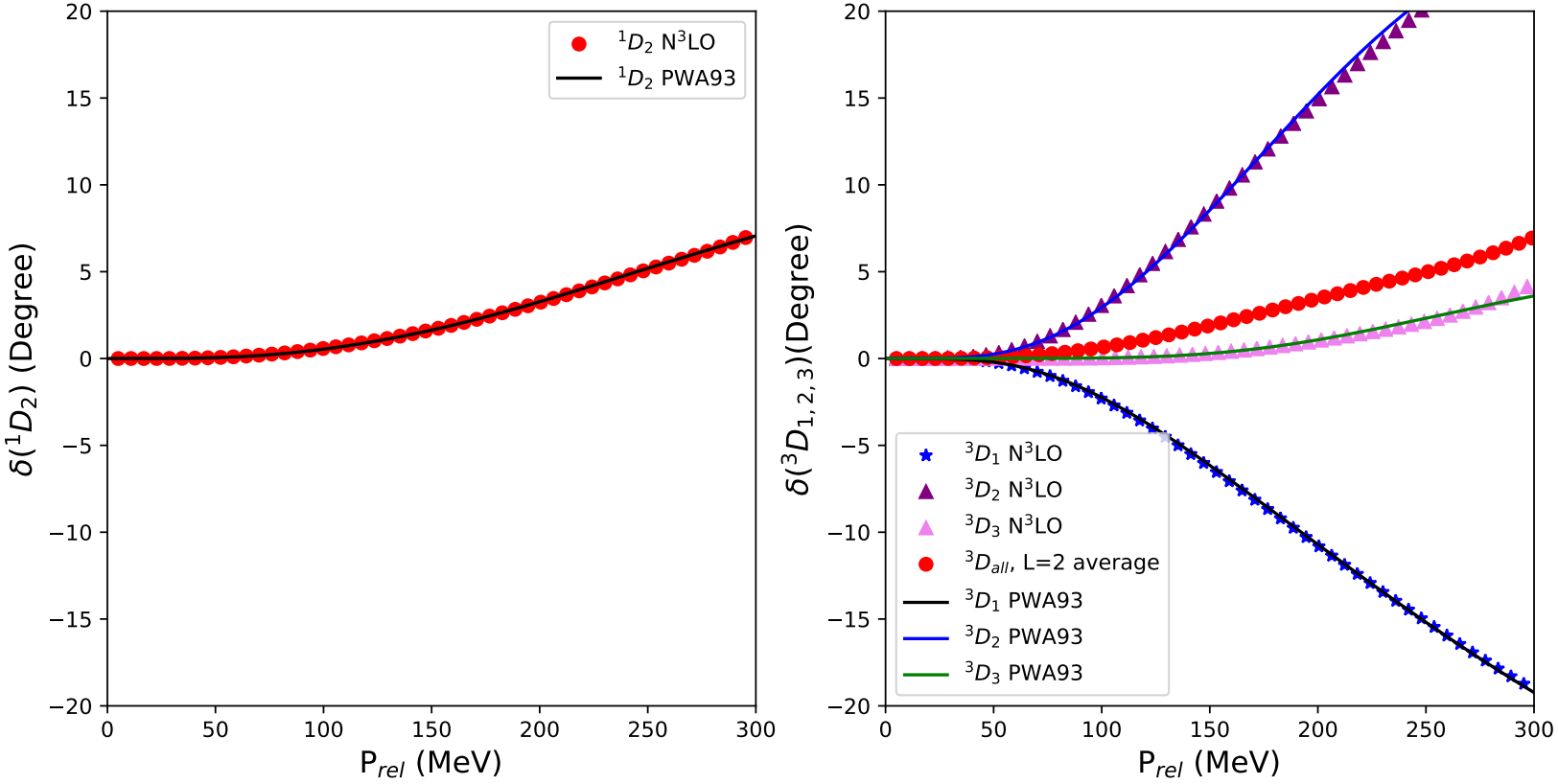

[D.L., Bogner, Brown, Elhatisari, Epelbaum, Hergert, Hjorth-Jensen, Krebs, Li, Lu, Meißner, PRL 127, 062501 (2021)]

Essential elements for nuclear binding

What is the minimal nuclear interaction that can reproduce the ground state properties of light nuclei, medium-mass nuclei, and neutron matter simultaneously with no more than a few percent error in the energies and charge radii?

We construct an interaction with only four parameters.

1. Strength of the two-nucleon S-wave interaction
2. Range of the two-nucleon S-wave interaction
3. Strength of three-nucleon contact interaction

fit to $A = 2$, 3 systems

4. Range of the local part of the two-nucleon interaction

fit to A > 3

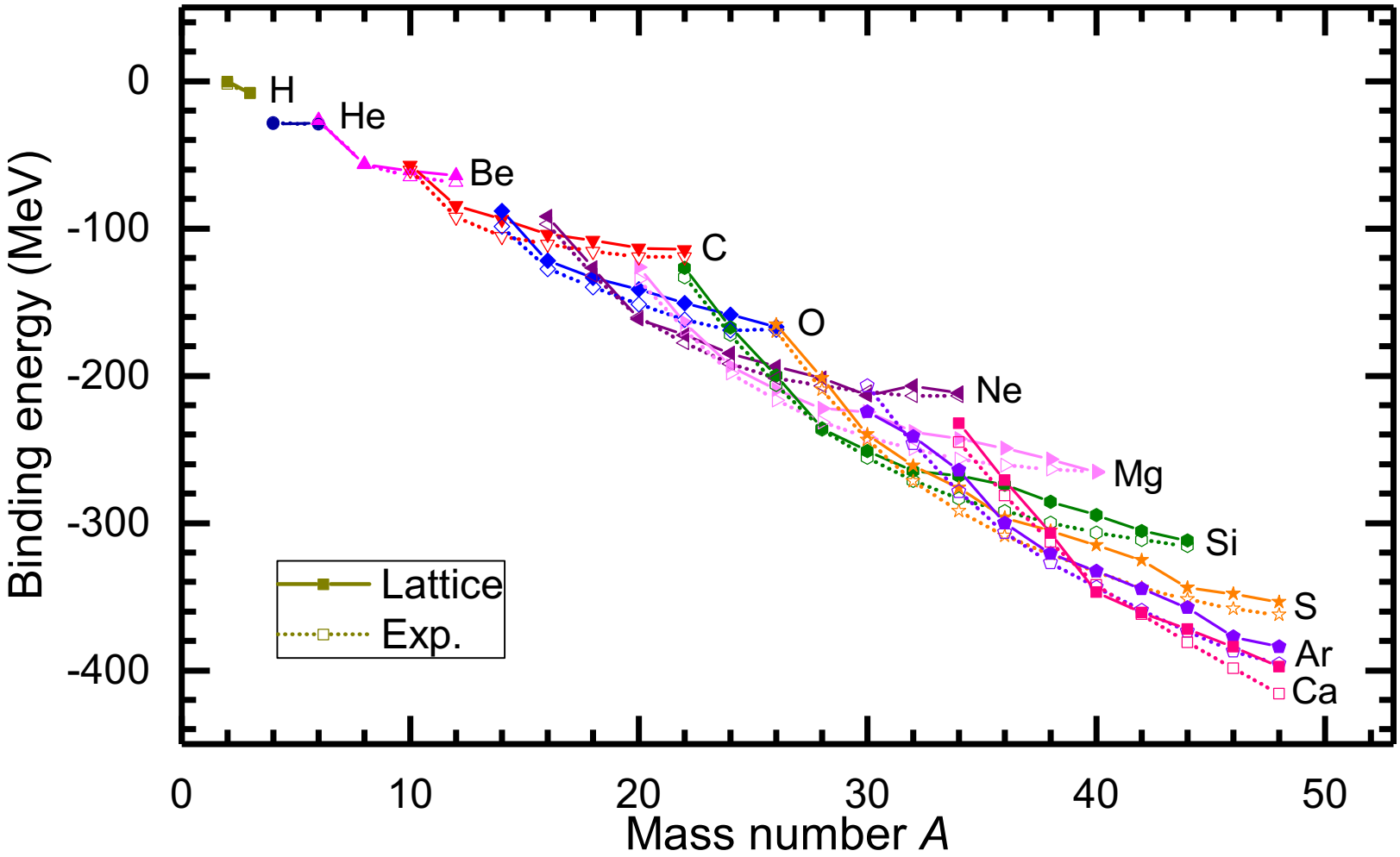

[Lu, Li, Elhatisari, D.L., Epelbaum, Meißner, PLB 797, 134863 (2019)]

	B	Exp.	$R_{\rm ch}$	Exp.
^{3}H	8.48(2)(0)	8.48	1.90(1)(1)	1.76
^{3}He	7.75(2)(0)	7.72	1.99(1)(1)	1.97
^{4}He	28.89(1)(1)	28.3	1.72(1)(3)	1.68
^{16}O	121.9(1)(3)	127.6	2.74(1)(1)	2.70
^{20}Ne	161.6(1)(1)	160.6	2.95(1)(1)	3.01
^{24}Mg	193.5(02)(17)	198.3	3.13(1)(2)	3.06
^{28}Si	235.8(04)(17)	236.5	3.26(1)(1)	3.12
^{40}Ca	346.8(6)(5)	342.1	3.42(1)(3)	3.48

Pinhole algorithm

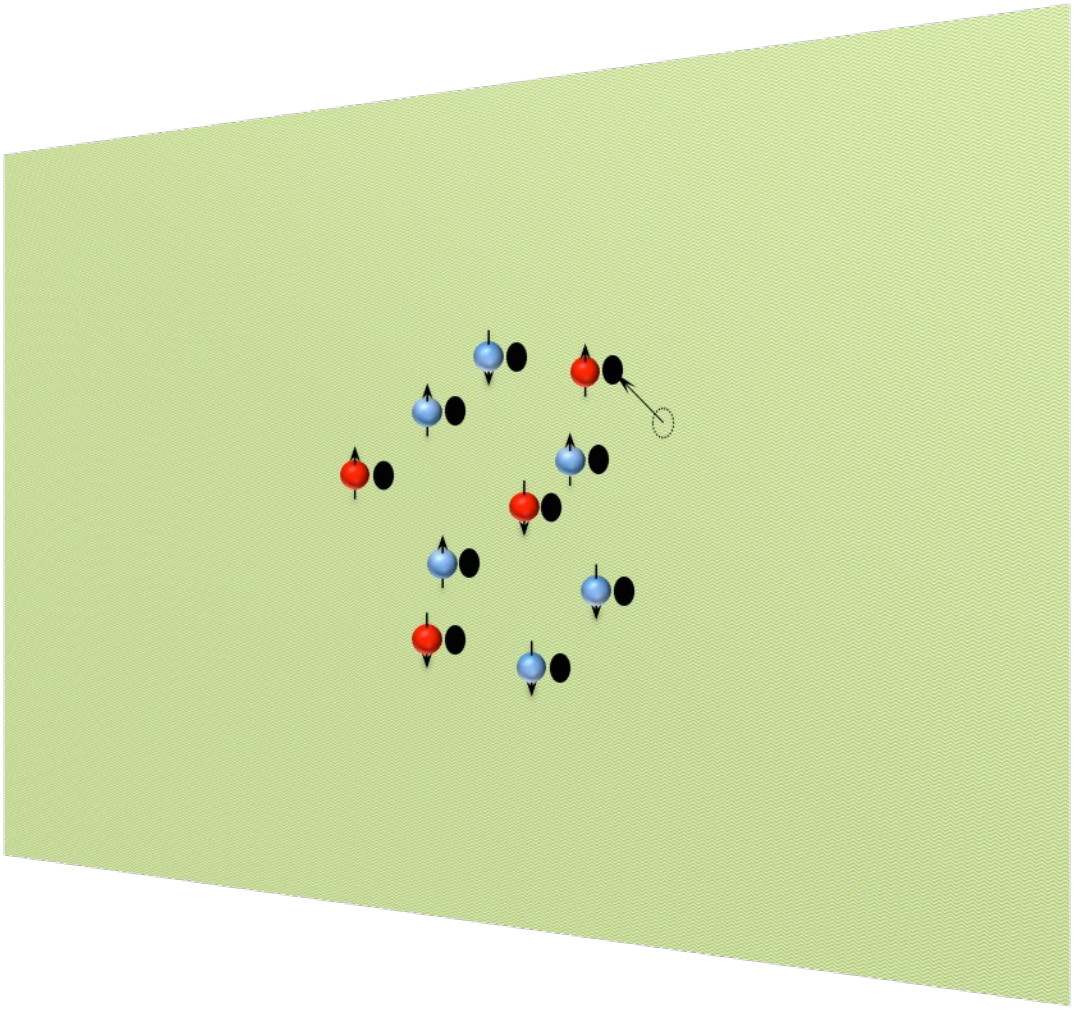

Seeing Structure with Pinholes

Consider the density operator for nucleon with spin i and isospin j

$$\rho_{i,j}(\mathbf{n}) = a^{\dagger}_{i,j}(\mathbf{n}) a_{i,j}(\mathbf{n})$$

We construct the normal-ordered A-body density operator

$$\rho_{i_1,j_1,\cdots i_A,j_A}(\mathbf{n}_1,\cdots \mathbf{n}_A) = :\rho_{i_1,j_1}(\mathbf{n}_1)\cdots\rho_{i_A,j_A}(\mathbf{n}_A):$$

In the simulations we do Monte Carlo sampling of the amplitude

$$A_{i_1,j_1,\cdots i_A,j_A}(\mathbf{n}_1,\cdots \mathbf{n}_A,t) = \langle\Psi_I|e^{-Ht/2}\rho_{i_1,j_1,\cdots i_A,j_A}(\mathbf{n}_1,\cdots \mathbf{n}_A)e^{-Ht/2}|\Psi_I\rangle$$

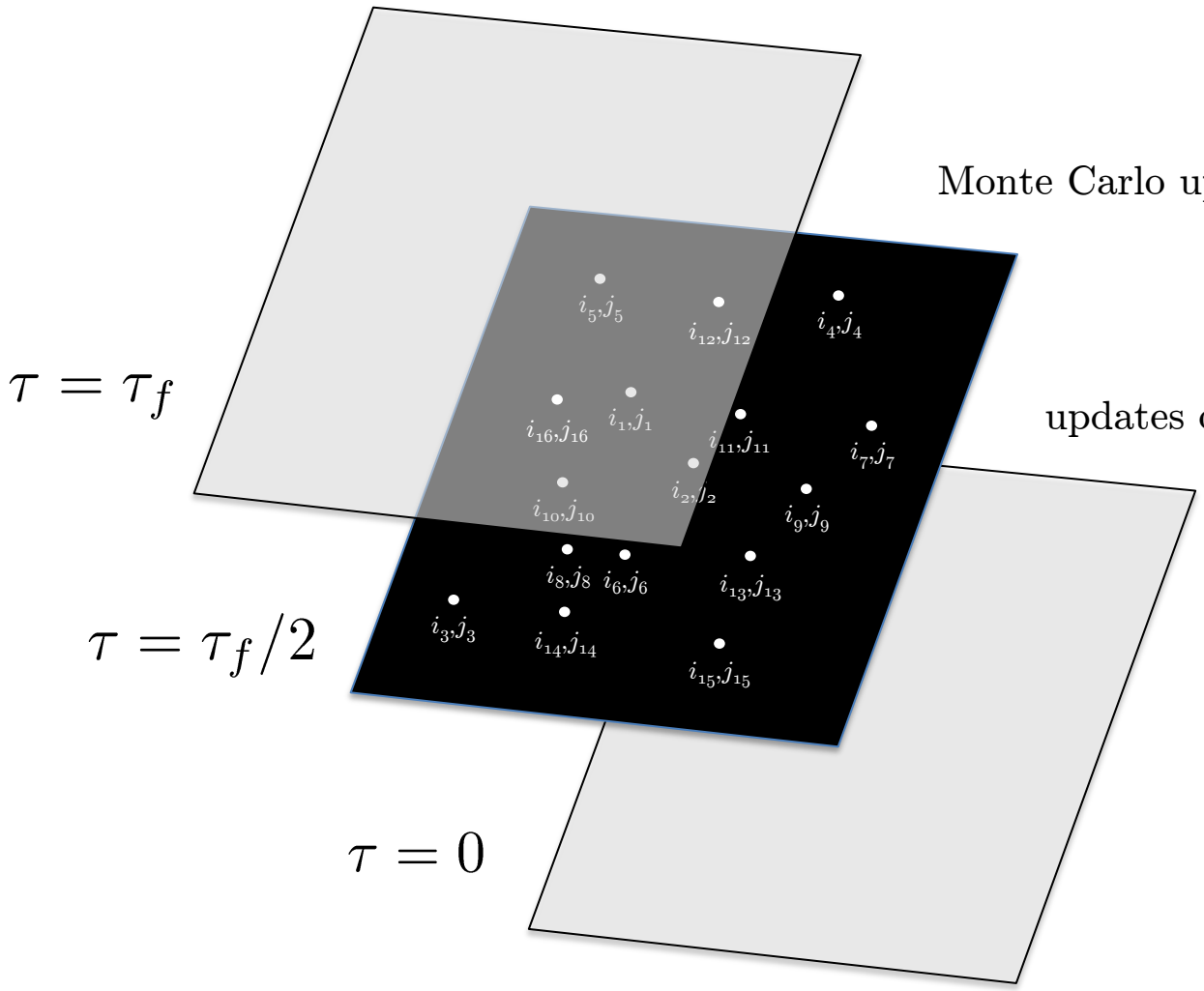

Monte Carlo updates of pinholes

Monte Carlo
updates of auxiliary/pion fields

]Elhatisari, Epelbaum, Krebs, Lähde, D.L., Li, Lu, Meißner, Rupak, PRL 119, 222505 (2017)]

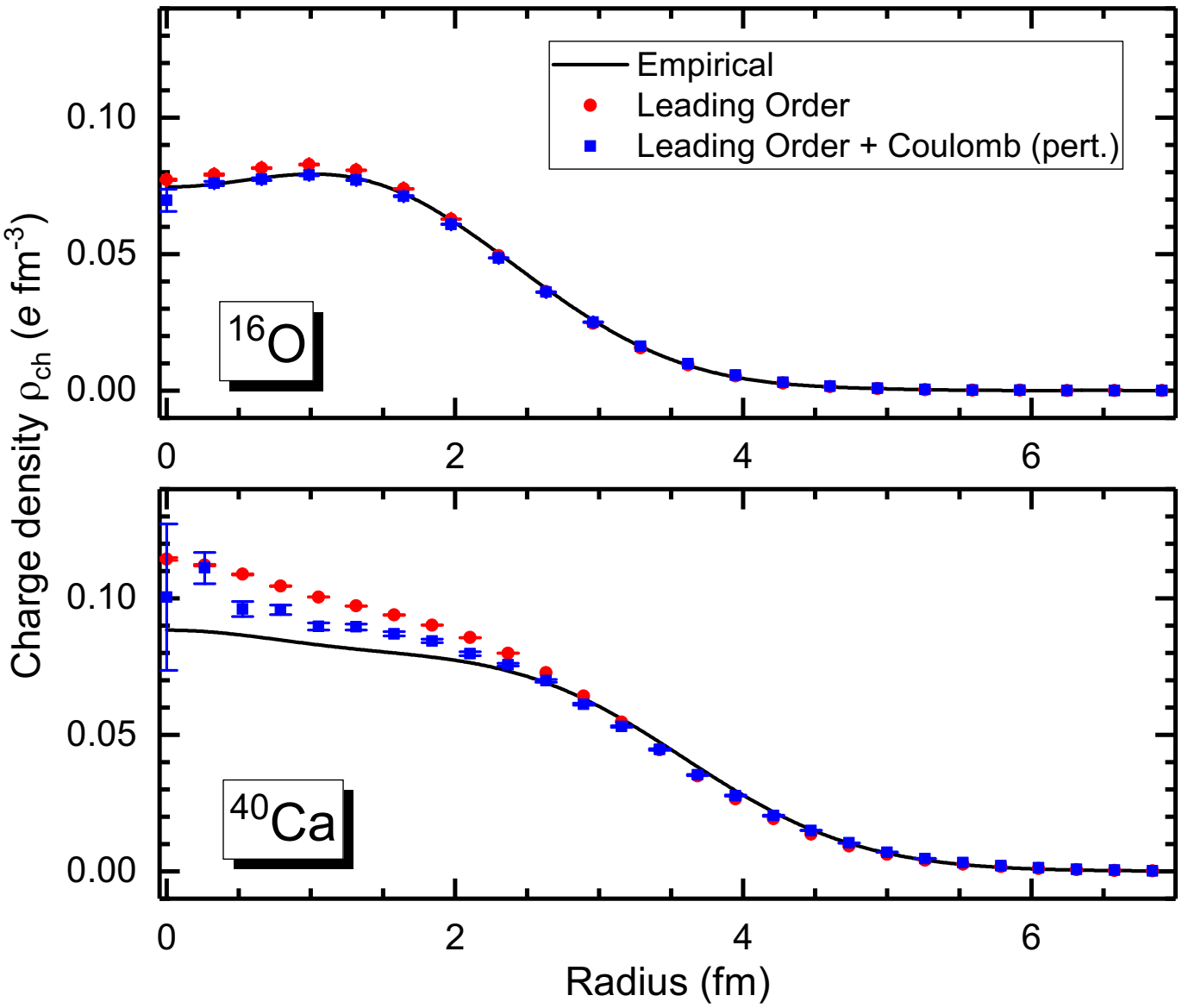

[Lu, Li, Elhatisari, D.L., Epelbaum, Meißner, PLB 797, 134863 (2019)]

^{16}O

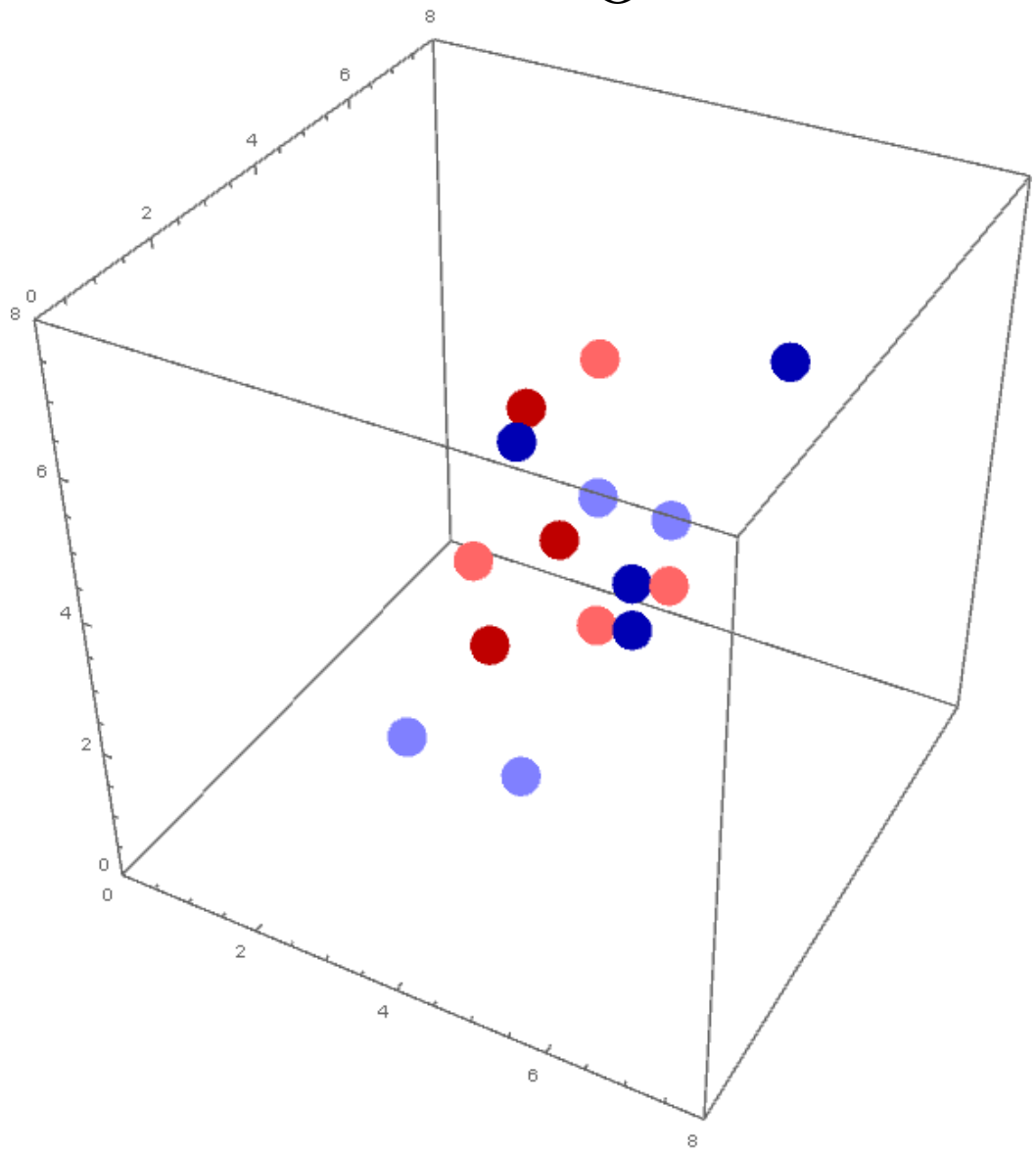

proton up
proton down
neutron up
neutron down

^{16}O ^{16}O collisions at RHIC and LHC energies

[Summerfield, Lu, Plumberg, D.L., Noronha-Hostler, Timmins PRC 104, L041901 (2021)]

^{16}O ^{16}O collisions have been proposed at RHIC and LHC to probe dependence on initial states of intermediate size, where alpha clustering is expected to be significant.

For ^{16}O ^{16}O collisions, the system is quite small, and we are pushing the limits of hydrodynamics. We use the Duke Bayesian tune of iEBE-VISHNU package to *p*Pb and PbPb collisions at the LHC.
[Bernhard et al., Nat. Phys. 15 1113 (2019), Moreland et al., Phys. Rev. C 101, 024911 (2020)]

We use the T_RENTo model to general the initial entropy distribution.
[Moreland et al., Phys. Rev. C 92, 044903 (2015)]

The initial entropy distribution is then passed through a free-streaming phase of duration 0.37 fm/c and used to initialize the hydrodynamics evolution.

We compute the following cumulants of the flow harmonics v_n:

$$v_n\{2\} = \left[\left\langle v_n^2 \right\rangle\right]^{\frac{1}{2}}$$
$$v_n\{4\} = \left[2\left\langle v_n^2 \right\rangle^2 - \left\langle v_n^4 \right\rangle\right]^{\frac{1}{4}}$$

We first compute results taking the initial density as a Woods-Saxon potential with density, radius, and diffusive fitted to empirical values. We then consider the same Woods-Saxon potential, taking into account the quark substructure of the nucleons. Lastly, we consider using the nucleon distribution from the lattice effective field theory calculations. This will incorporate correlations such as alpha clustering.

[Summerfield, Lu, Plumberg, D.L., Noronha-Hostler, Timmins PRC 104, L041901 (2021)]

How much alpha clustering?

$$\left\langle \rho^2 \right\rangle_{^{16}\mathrm{O}} = 4.59(11) \left\langle \rho^2 \right\rangle_{^{4}\mathrm{He}}$$
$$\left\langle \rho^3 \right\rangle_{^{16}\mathrm{O}} = 4.67(23) \left\langle \rho^3 \right\rangle_{^{4}\mathrm{He}}$$
$$\left\langle \rho^4 \right\rangle_{^{16}\mathrm{O}} = 4.44(27) \left\langle \rho^4 \right\rangle_{^{4}\mathrm{He}}$$

About 10% greater than the simple tensor product of four alpha clusters. The excess is due to entanglement of the alpha cluster wave functions.

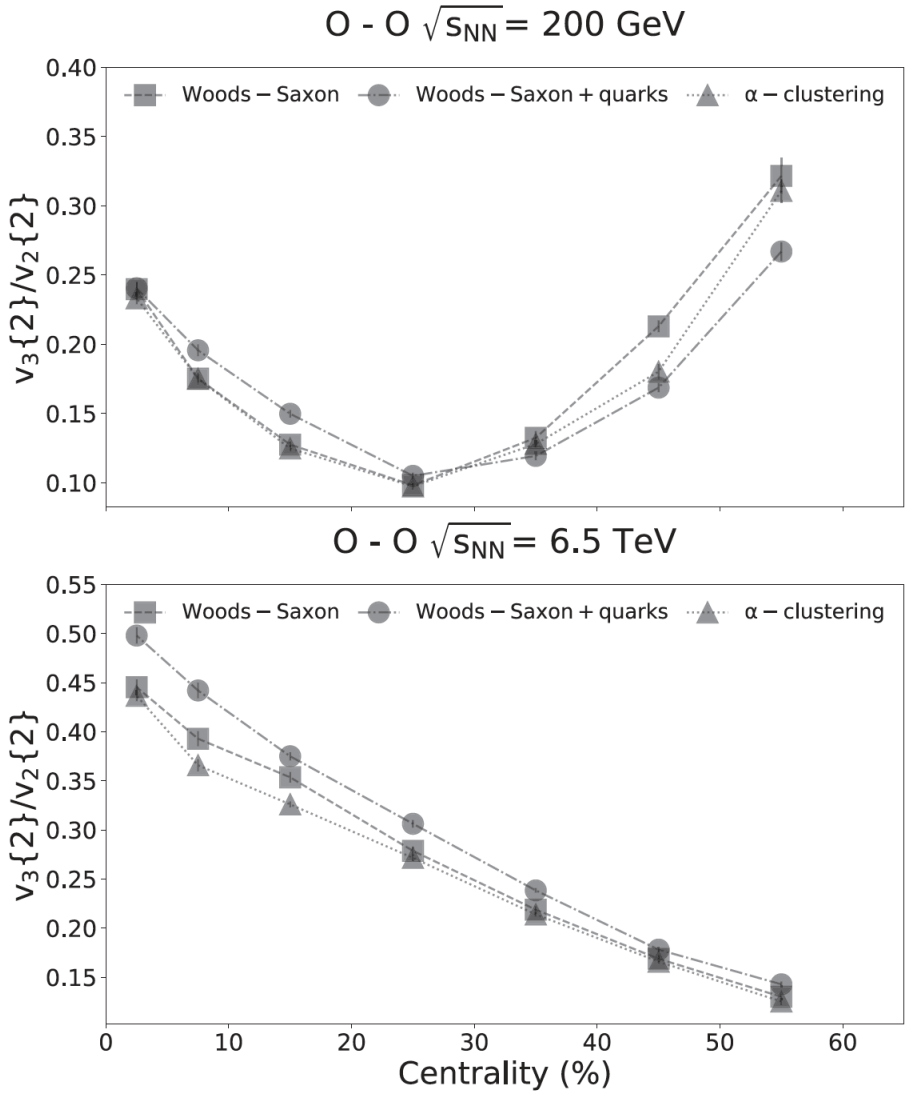

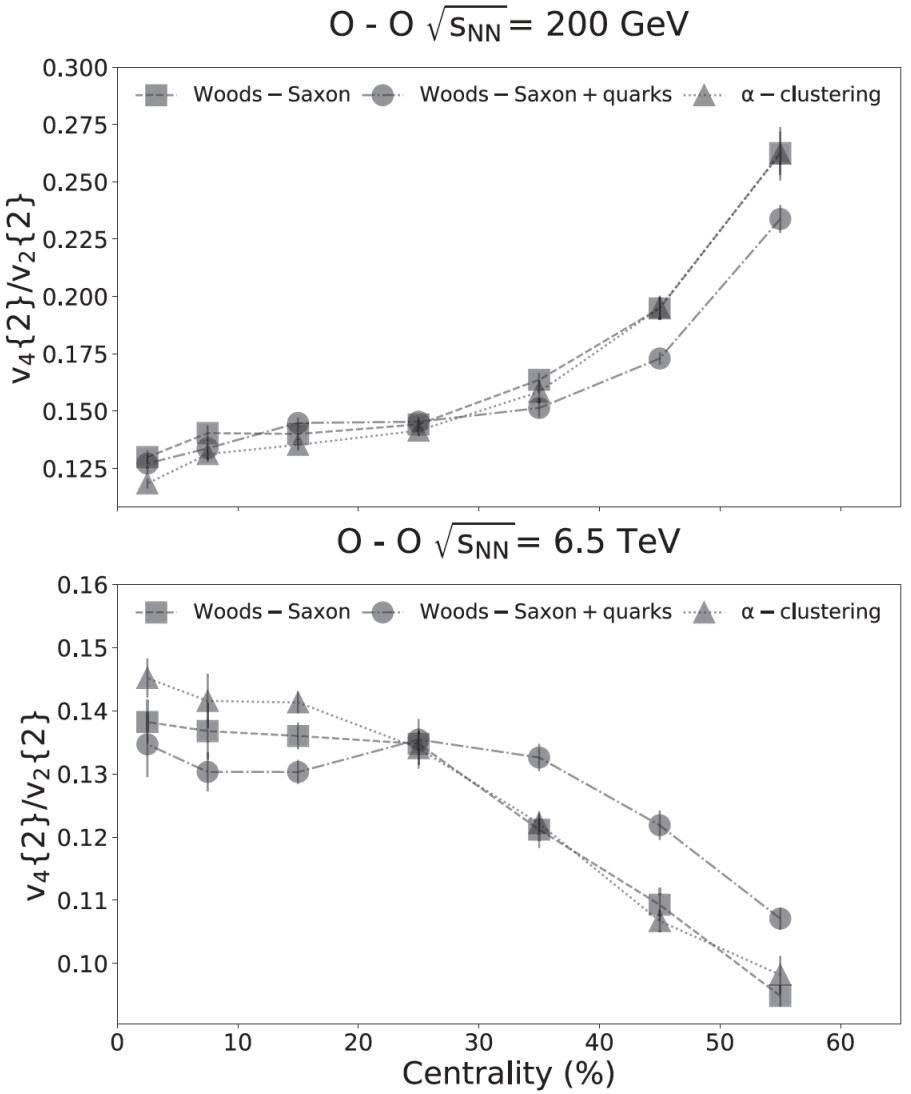

[Summerfield, Lu, Plumberg, D.L., Noronha-Hostler, Timmins PRC 104, L041901 (2021)]

Ab initio nuclear thermodynamics

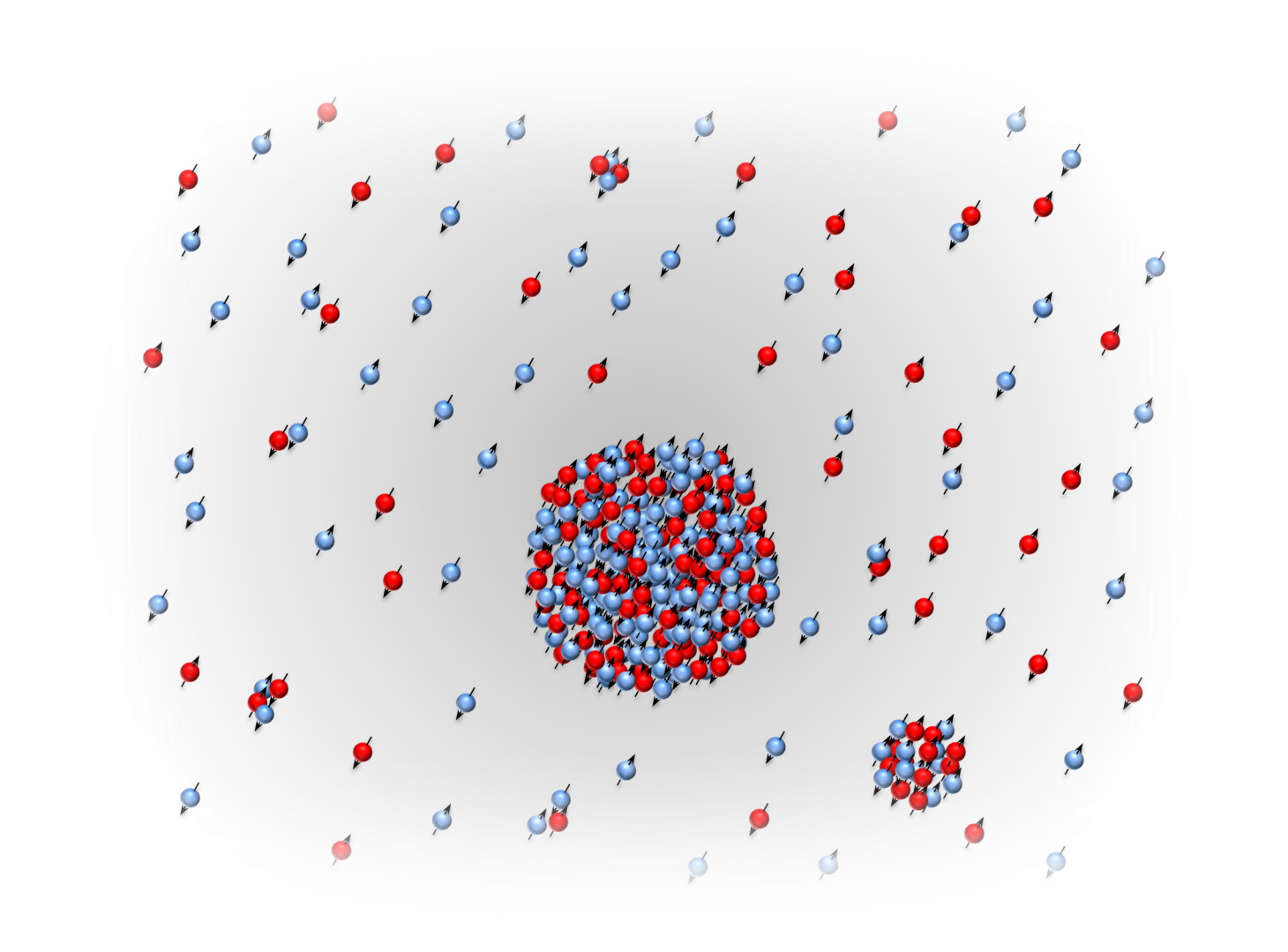

Ab initio nuclear thermodynamics

In order to compute thermodynamic properties of finite nuclei, nuclear matter, and neutron matter, we need to compute the partition function

$$\mathrm{Tr}\exp(-\beta H)$$

We compute the quantum mechanical trace over A-nucleon states by summing over pinholes (position eigenstates) for the initial and final states

$$\mathrm{Tr}\,O = \frac{1}{A!}\sum_{i_1\cdots i_A, j_1\cdots j_A, \mathbf{n}_1\cdots\mathbf{n}_A} \langle 0|a_{i_A,j_A}(\mathbf{n}_A)\cdots a_{i_1,j_1}(\mathbf{n}_1)\,O\,a^\dagger_{i_1,j_1}(\mathbf{n}_1)\cdots a^\dagger_{i_A,j_A}(\mathbf{n}_A)|0\rangle$$

This can be used to calculate the partition function in the canonical ensemble.

[Lu, Li, Elhatisari, D.L., Drut, Lähde, Epelbaum, Meißner, PRL 125, 192502 (2020)]

Metropolis updates of pinholes

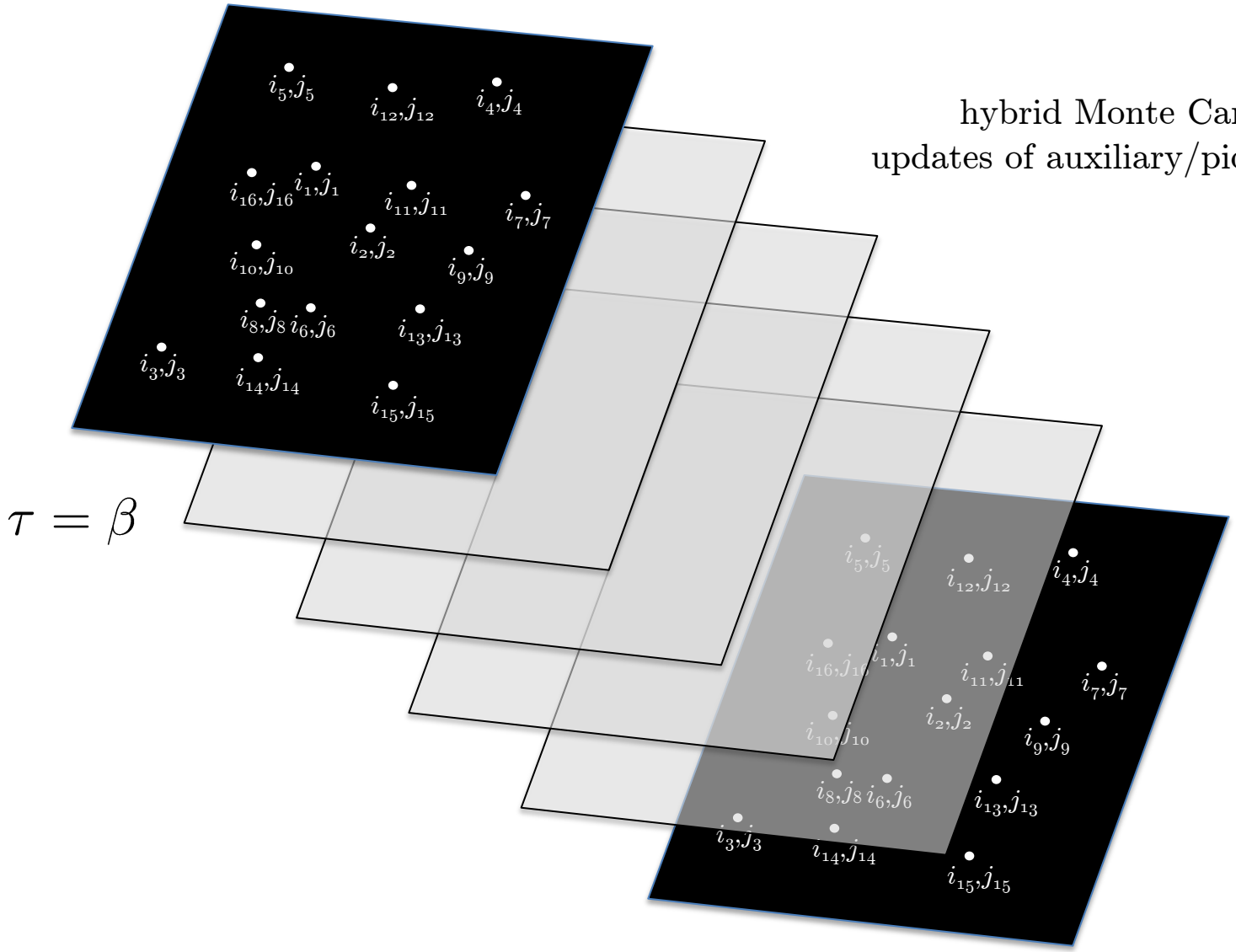

hybrid Monte Carlo
updates of auxiliary/pion fields

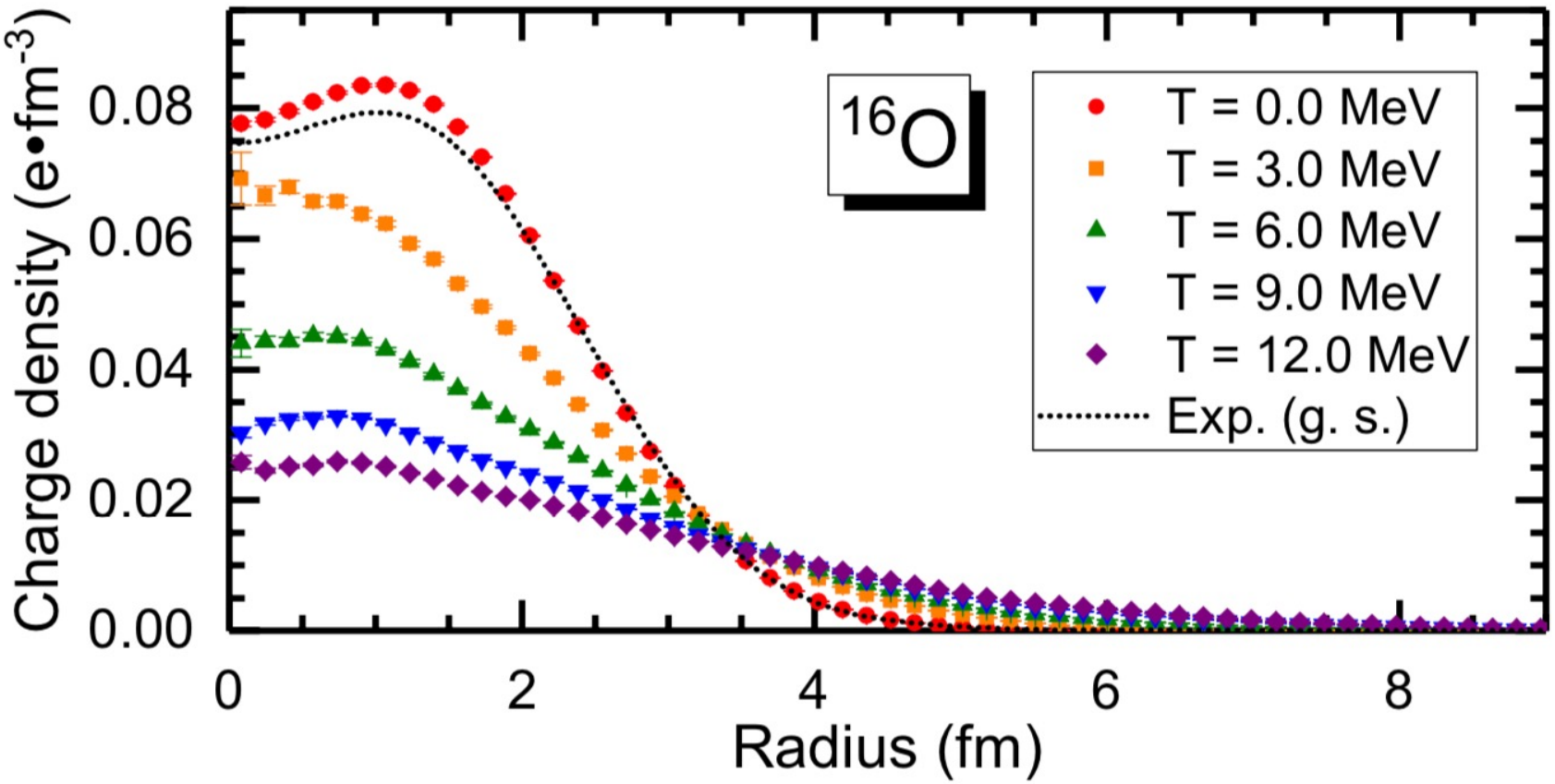
Charge density (e•fm^{-3})
0.08
0.06
0.04
0.02
0.00
0
2
4
6
8
Radius (fm)
^{16}O
T = 0.0 MeV
T = 3.0 MeV
T = 6.0 MeV
T = 9.0 MeV
T = 12.0 MeV
Exp. (g. s.)

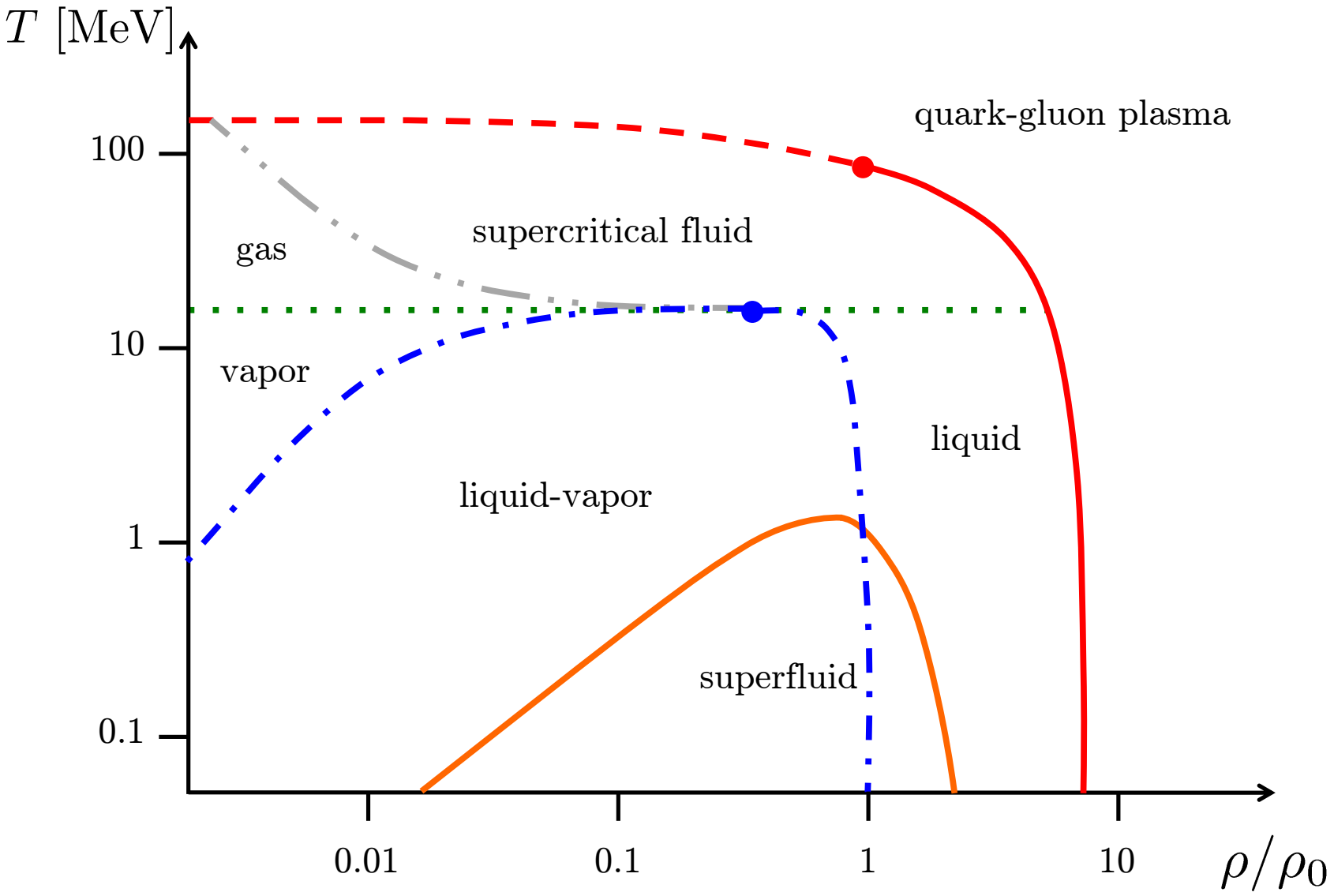
T [MeV]
100
10
1
0.1
quark-gluon plasma
supercritical fluid
gas
vapor
liquid
liquid-vapor
superfluid
0.01
0.1
1
10
ρ/ρ_0

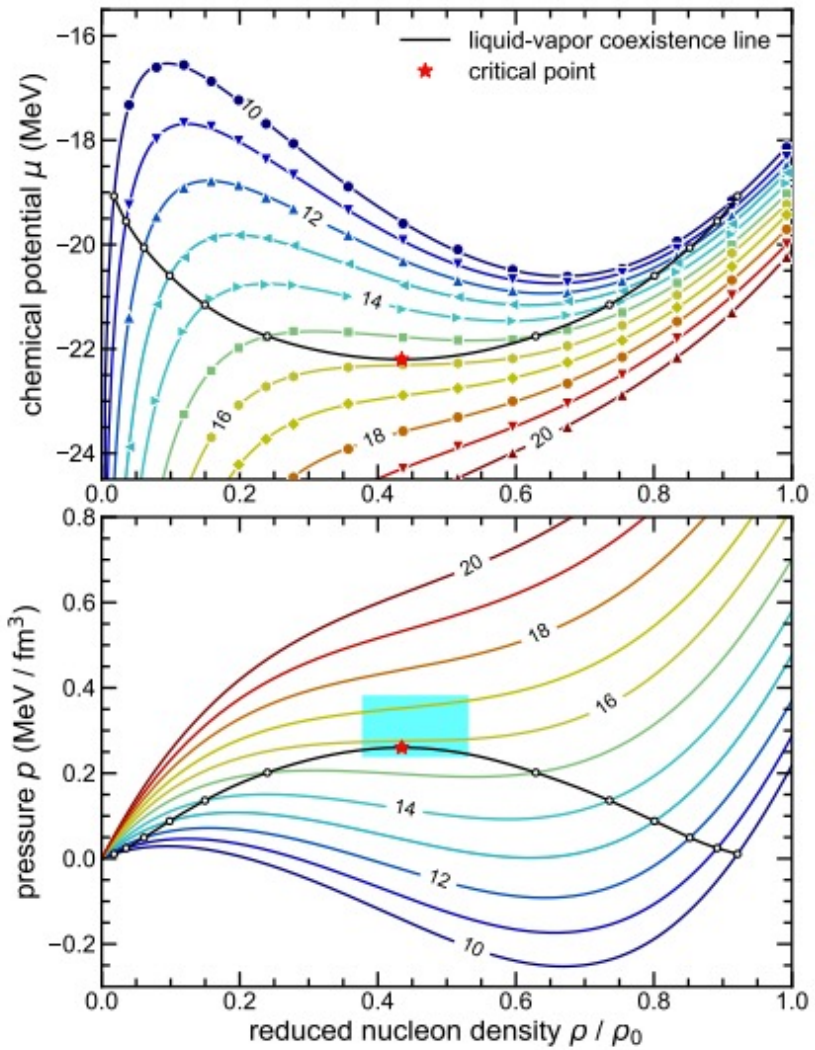

$$T_c = 15.80(0.32)(1.60)\,\mathrm{MeV}$$
$$\rho_c = 0.089(04)(18)\,\mathrm{fm}^{-3}$$
$$\mu_c = -22.20(0.44)(2.20)\,\mathrm{MeV}$$
$$P_c = 0.260(05)(30)\,\mathrm{MeV\ fm}^{-3}$$

[Lu, Li, Elhatisari, D.L., Drut, Lähde, Epelbaum, Meißner, PRL 125, 192502 (2020)]

Alpha clustering as function of density and temperature

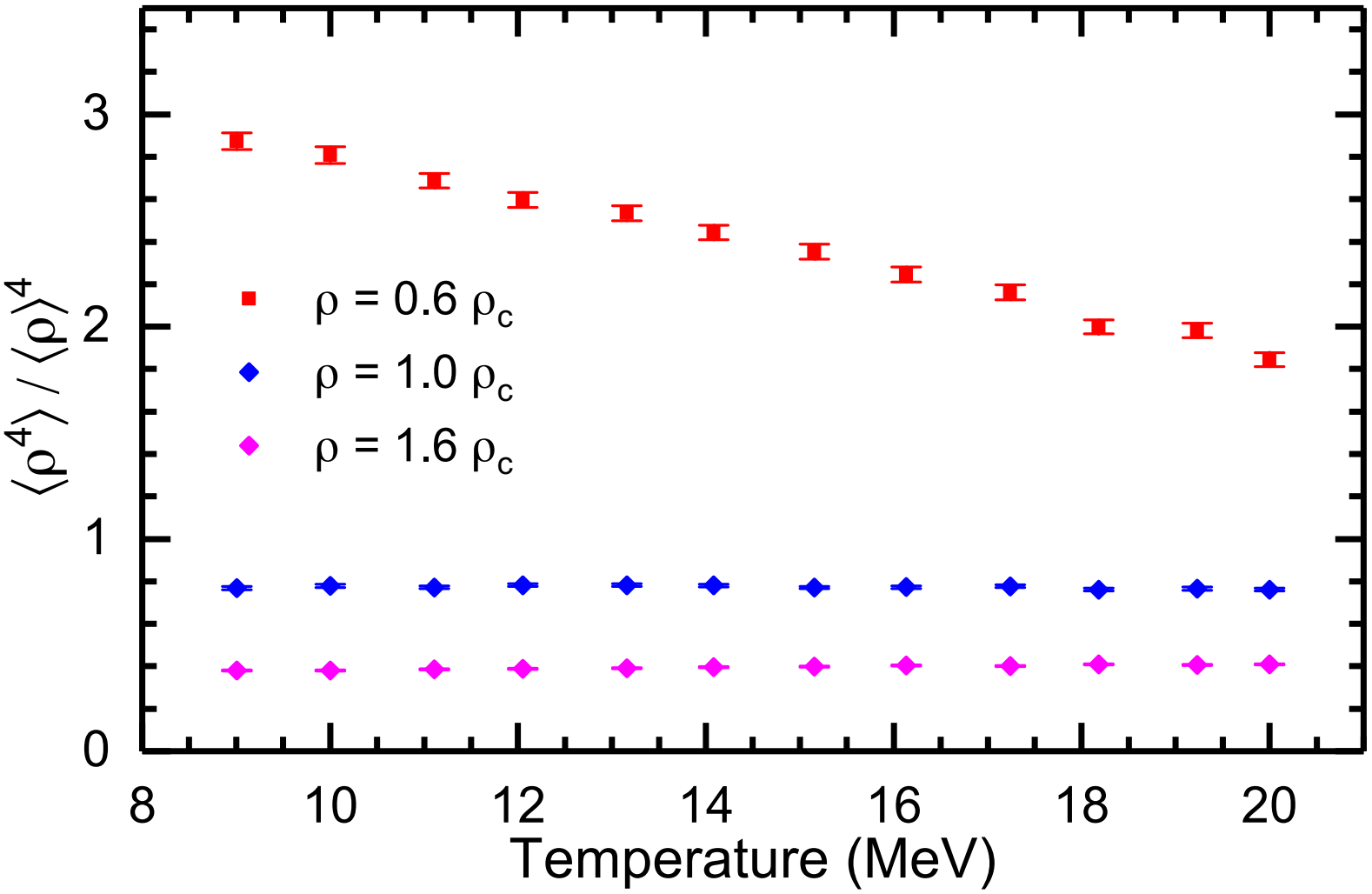

[Lu, Li, Elhatisari, D.L., Drut, Lähde, Epelbaum, Meißner, PRL 125, 192502 (2020)]

Structure and spectrum of ^{12}C

Shen, Lähde, D.L. Meißner, EPJA 57, 276 (2021)

State	$a = 1.97$ fm	$a = 1.64$ fm	Experiment
0_1^+	$-92.15(3)$	$-92.12(4)$	-92.162
2_1^+	$-88.87(4)$	$-88.19(17)$	-87.722
0_2^+	$-85.20(15)$	$-85.23(22)$	-84.508
3_1^-	$-84.9(2)$	$-83.3(5)$	$-82.521(5)$
2_2^+	$-83.5(2)$	$-83.1(5)$	$-82.29(6)$
0_3^+	$-80.0(3)$	$-79.2(6)$	$-81.9(3)$
1_1^-	$-81.5(4)$	$-79.7(4)$	$-81.315(4)$
2_1^-	$-78.6(2)$	$-76.1(2)$	$-80.326(4)$
1_1^+	$-79.67(11)$	$-78.14(24)$	$-79.452(6)$
4_1^-	$-78.1(2)$	$-75.5(5)$	$-78.846(20)$
4_1^+	$-80.99(11)$	$-79.1(6)$	$-78.083(5)$
2_3^+	$-79.9(4)$	$-77.9(2)$	-76.056
0_4^+	$-79.25(11)$	$-76.94(18)$	-74.402

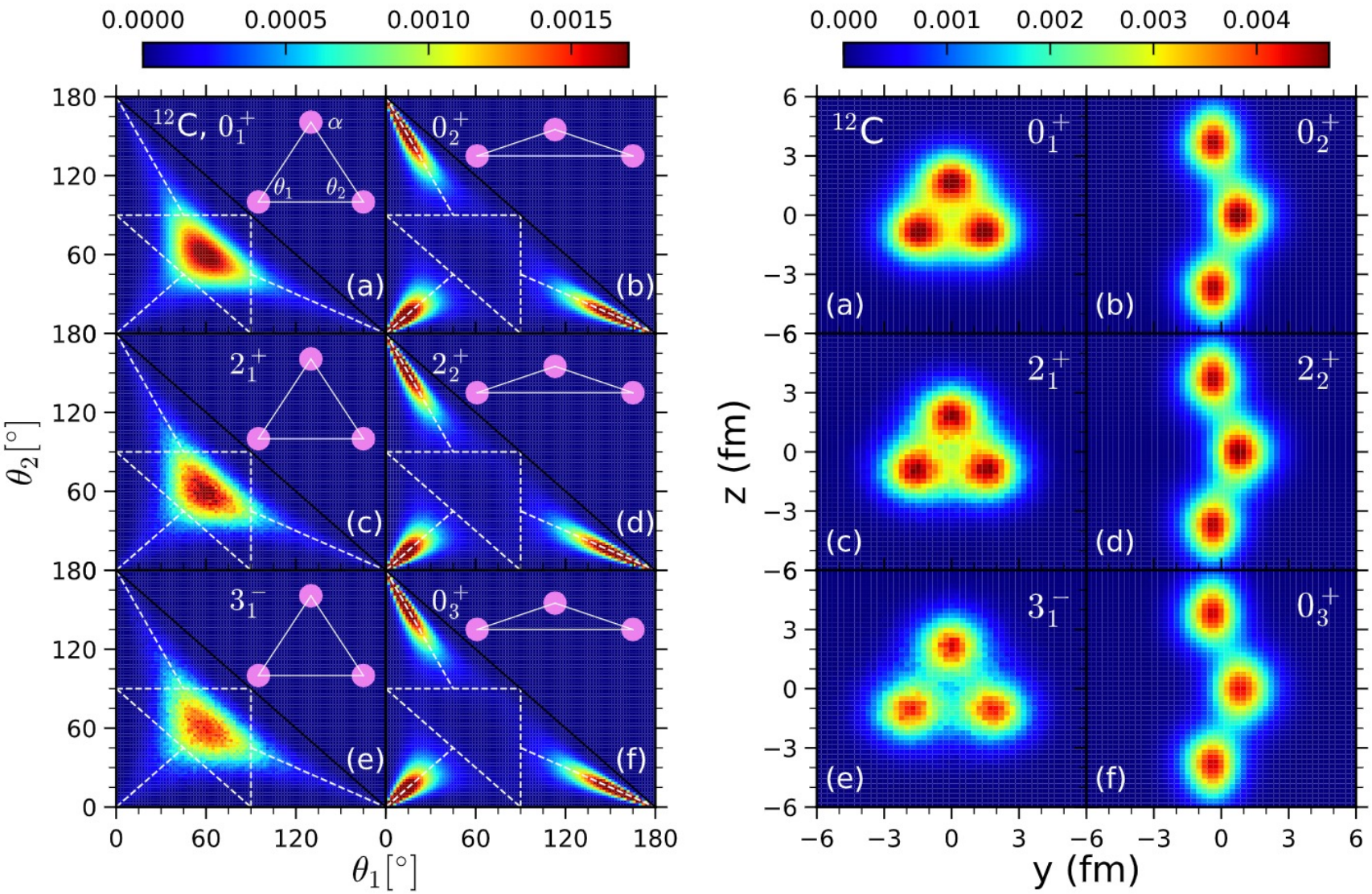

[Shen, Lähde, D.L. Meißner, arXiv:2202.13596]

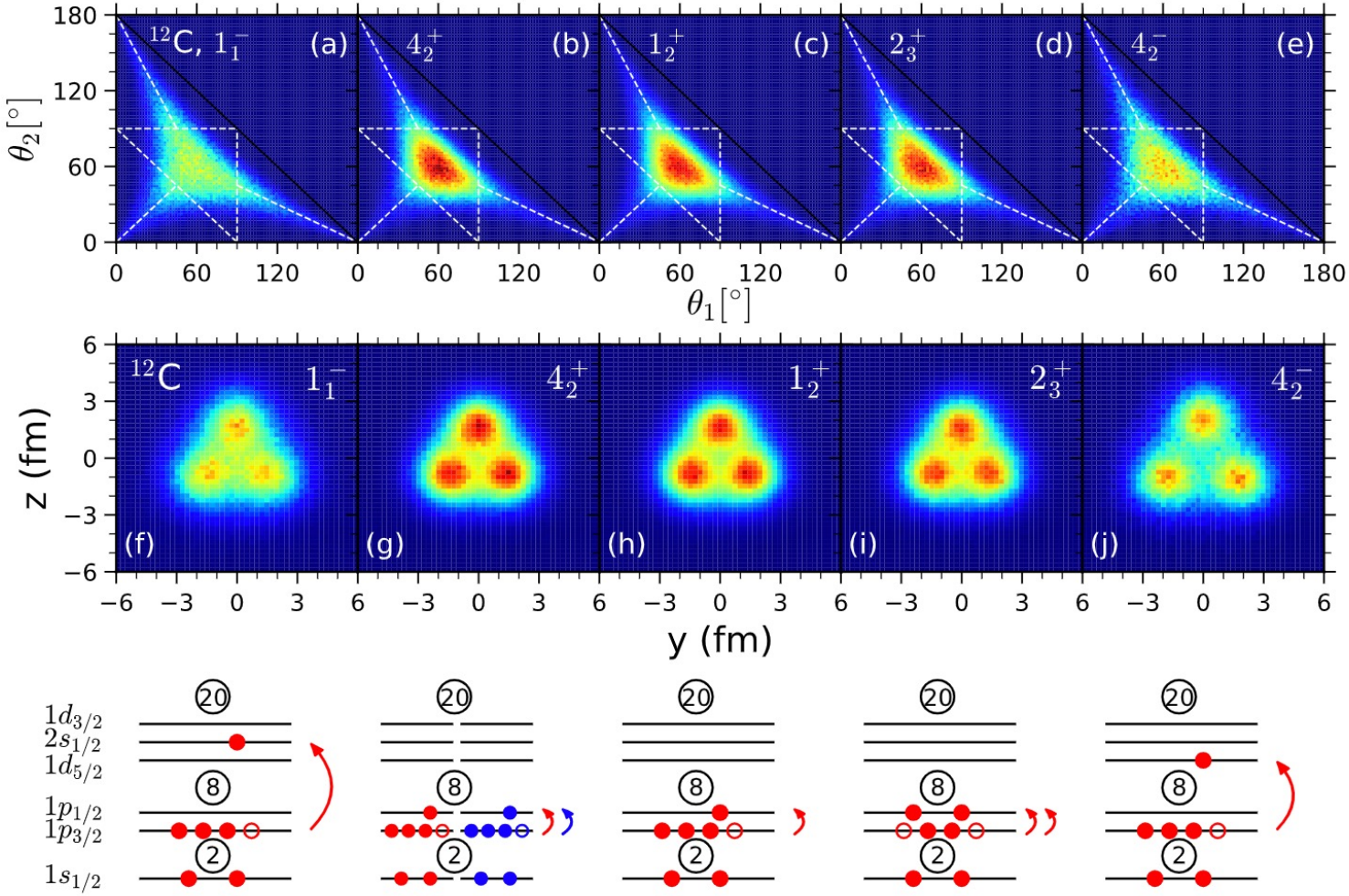

Figure S3: **Top Panel:** Density distribution for the two inner angles of the triangle formed by the three alpha clusters. **Middle Panel:** Tomographic projection of the nuclear density. **Lower Panel:** Sketch of the orbitals for the shell model initial states used in each of these calculations.

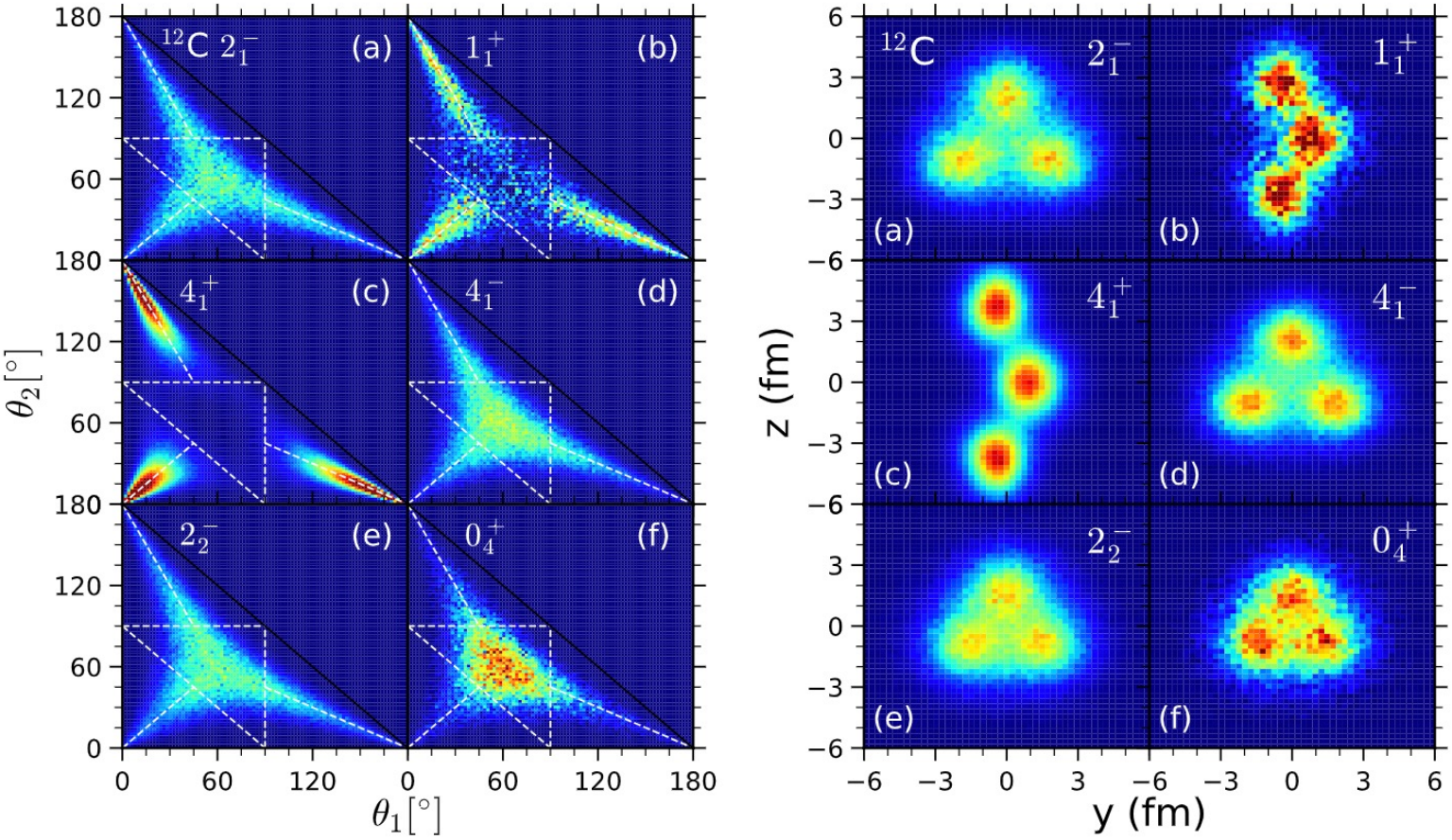

Figure S4: **Left Panel:** Density distribution for the two inner angles of the triangle formed by the three alpha clusters. **Right Panel:** Tomographic projection of the nuclear density. From (a) to (f), the selected states are ordered by their energies from low to high.

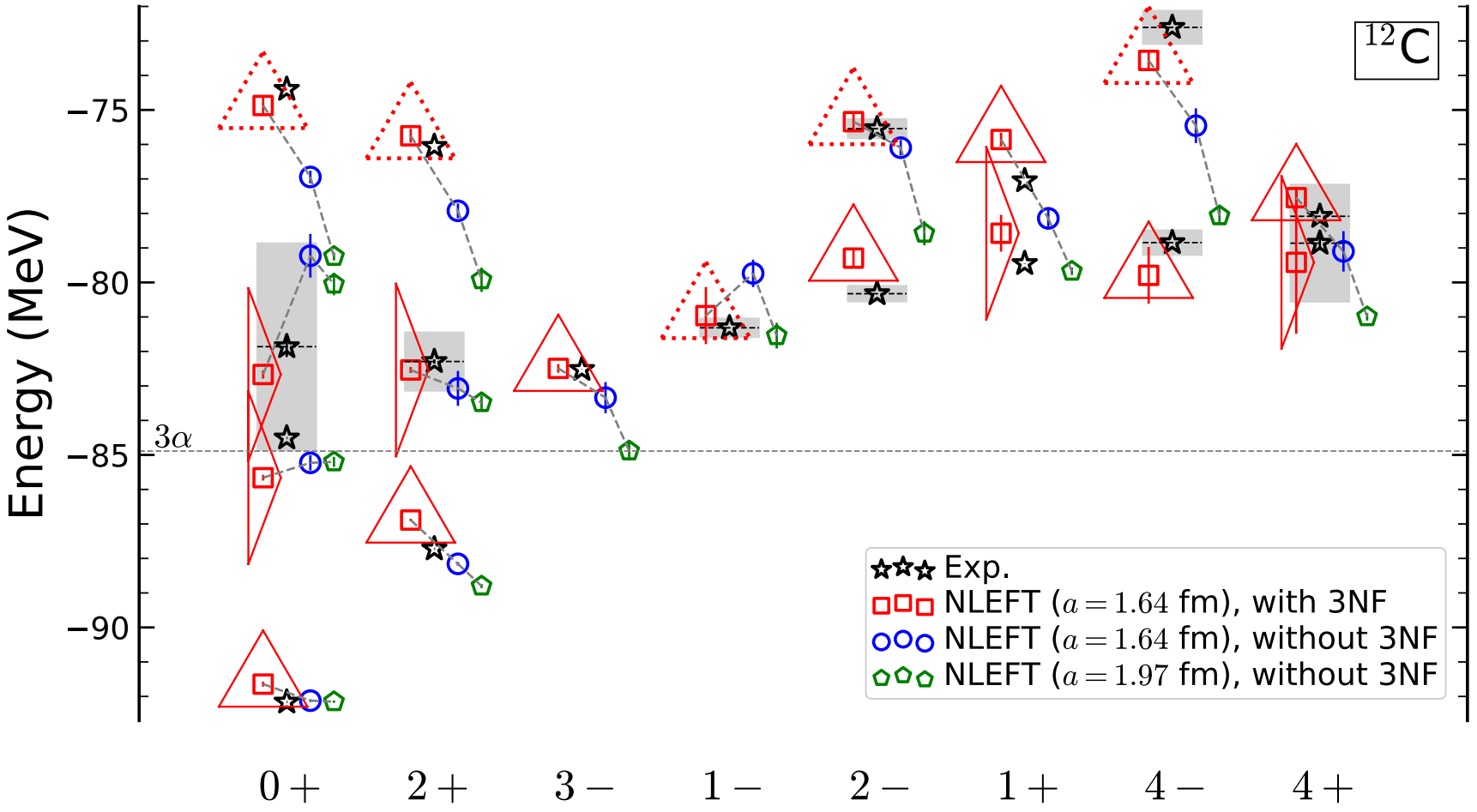

[Shen, Lähde, D.L. Meißner, arXiv:2202.13596]

Wave function matching

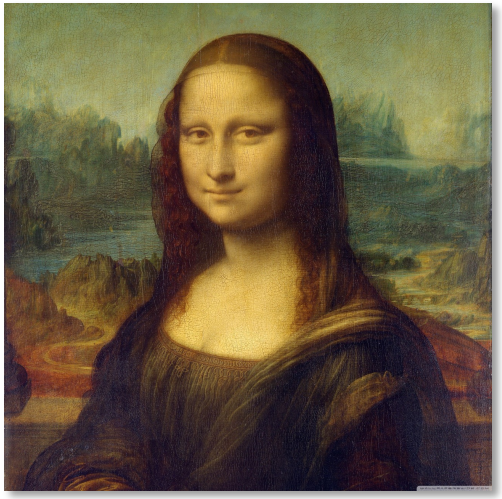

[Work in progress: Elhatisari, Bovermann, et al.]

Lattice Monte Carlo simulations can compute highly nontrivial correlations in nuclear many-body systems. Unfortunately, sign oscillations prevent direct simulations using a high-fidelity Hamiltonian based on chiral effective field theory due to short-range repulsion.

Wave function matching solves this problem by means of unitary transformations and perturbation theory. By using unitary transformations, we construct a high-fidelity Hamiltonian that can be reached by perturbation theory, starting from a Hamiltonian without a sign problem.

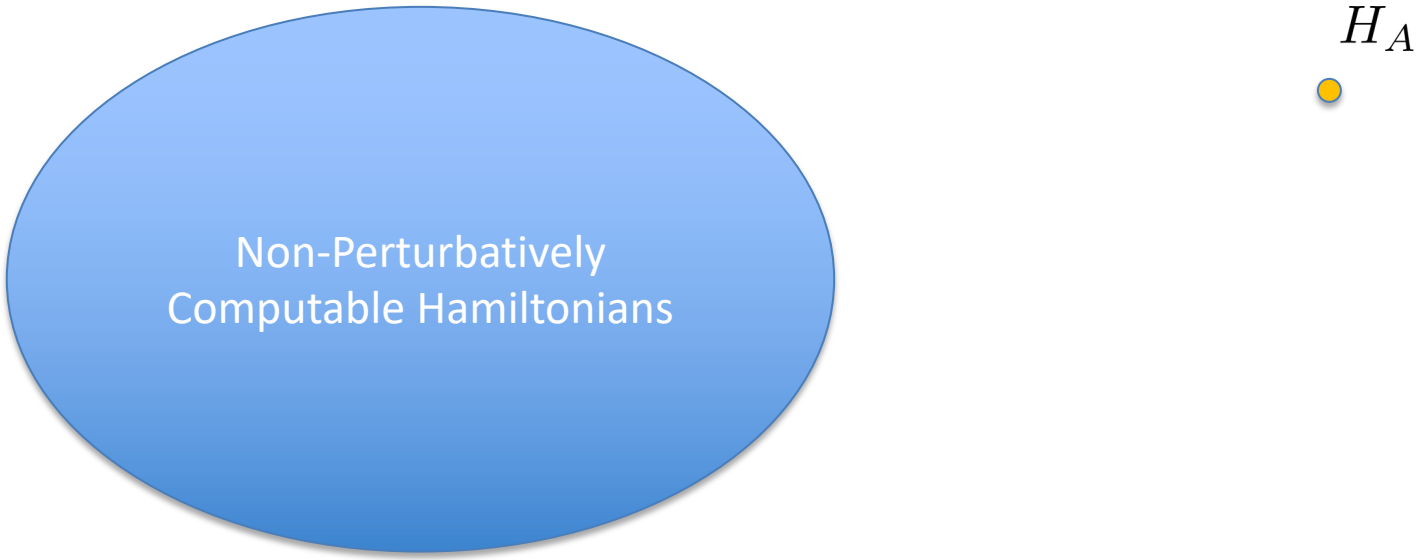
Non-Perturbatively
Computable Hamiltonians
H_A

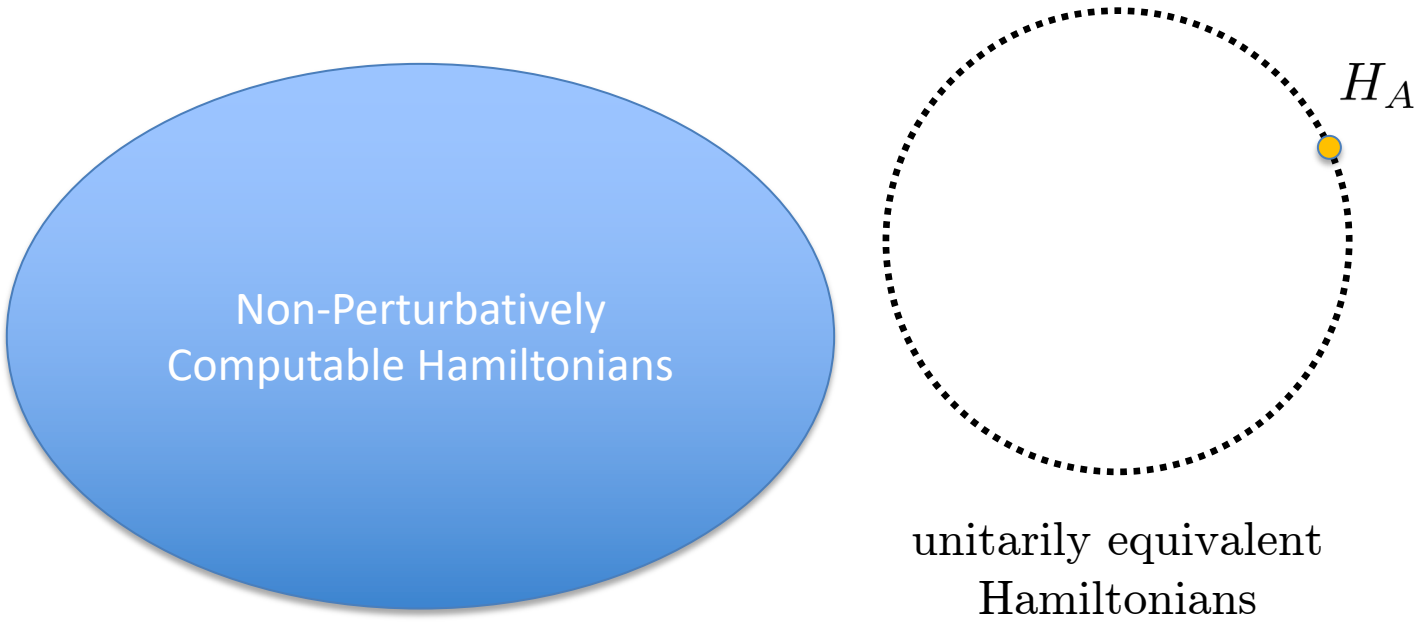
Non-Perturbatively
Computable Hamiltonians
H_A
unitarily equivalent
Hamiltonians

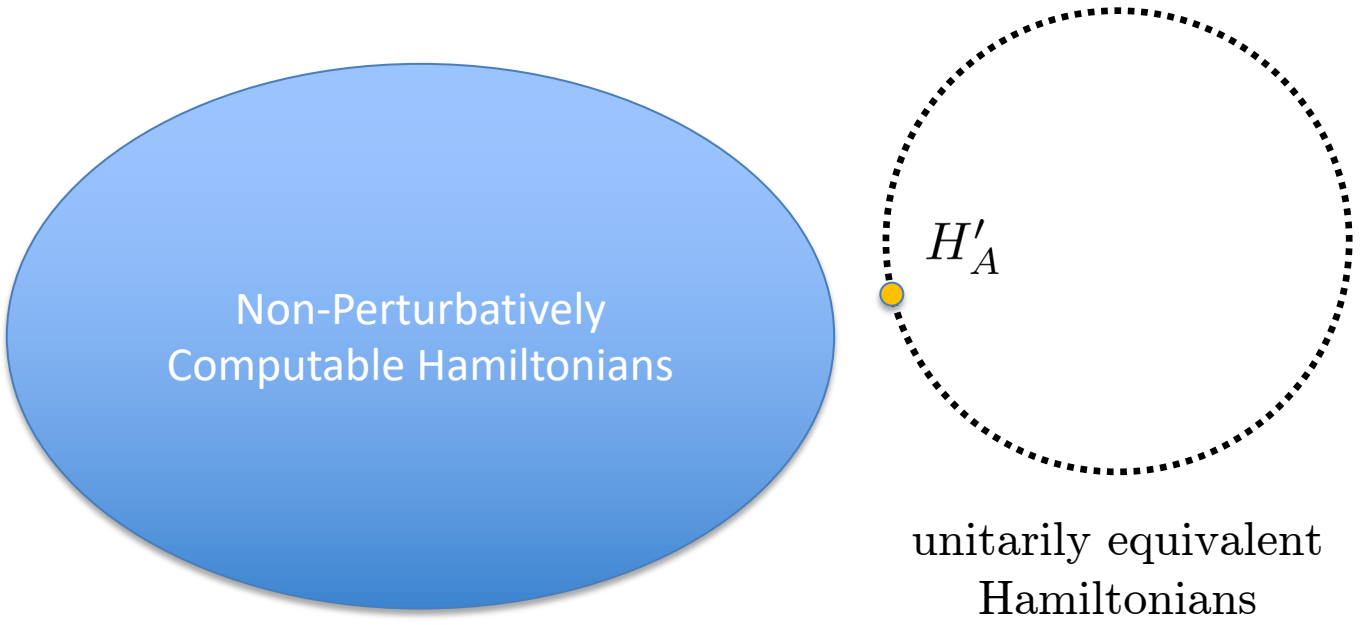
Non-Perturbatively
Computable Hamiltonians
H'_A
unitarily equivalent
Hamiltonians

Wave function matching

$V_A(r)$

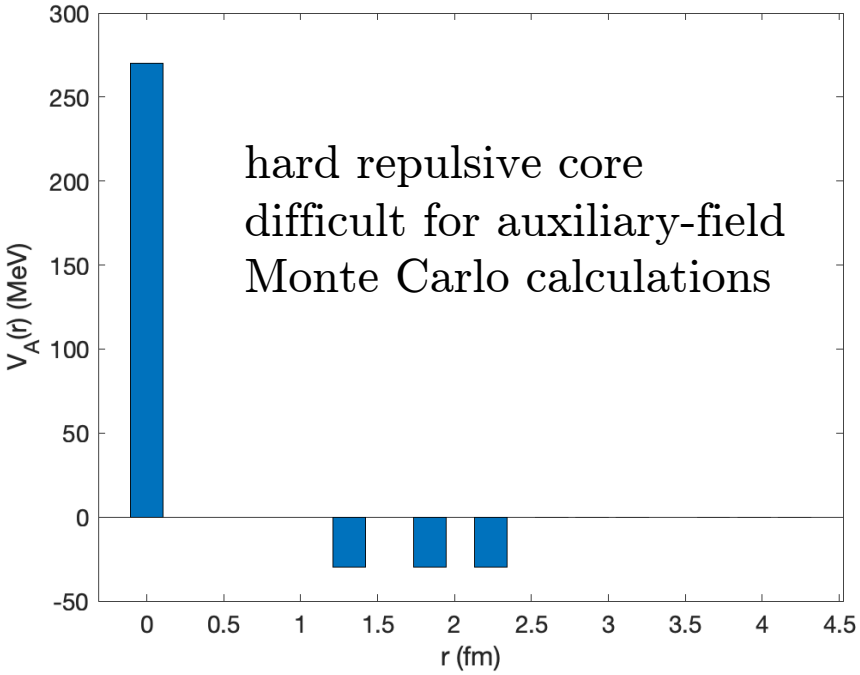

$V_B(r)$

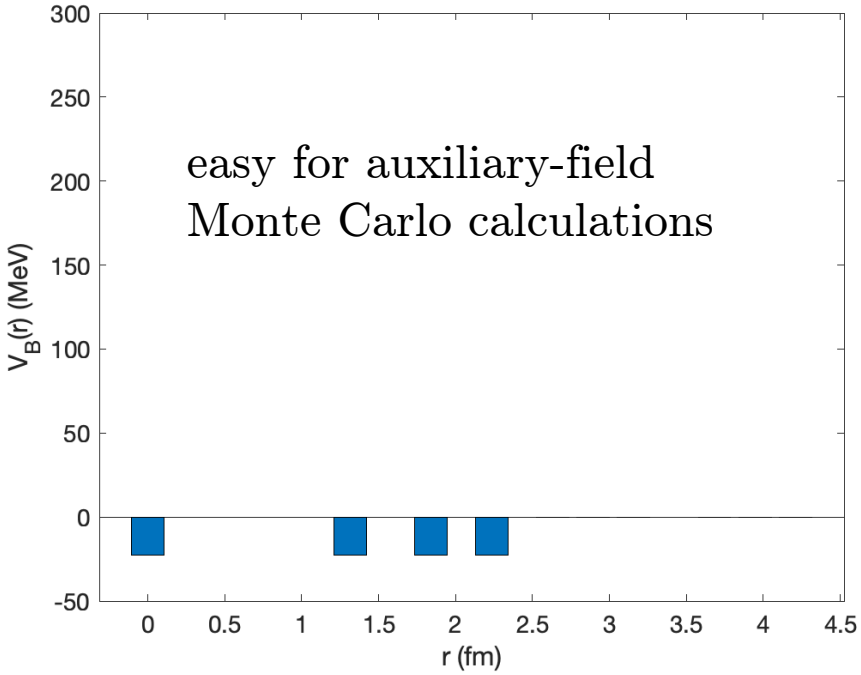

$V_A(r)$

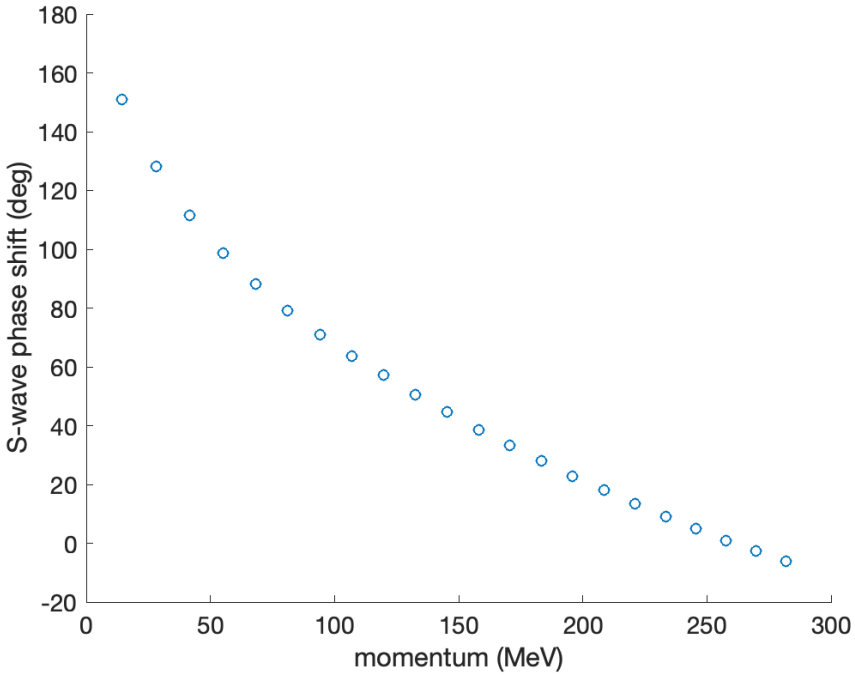
S-wave phase shift (deg)
momentum (MeV)
180
160
140
120
100
80
60
40
20
0
-20
0
50
100
150
200
250
300

$V_B(r)$

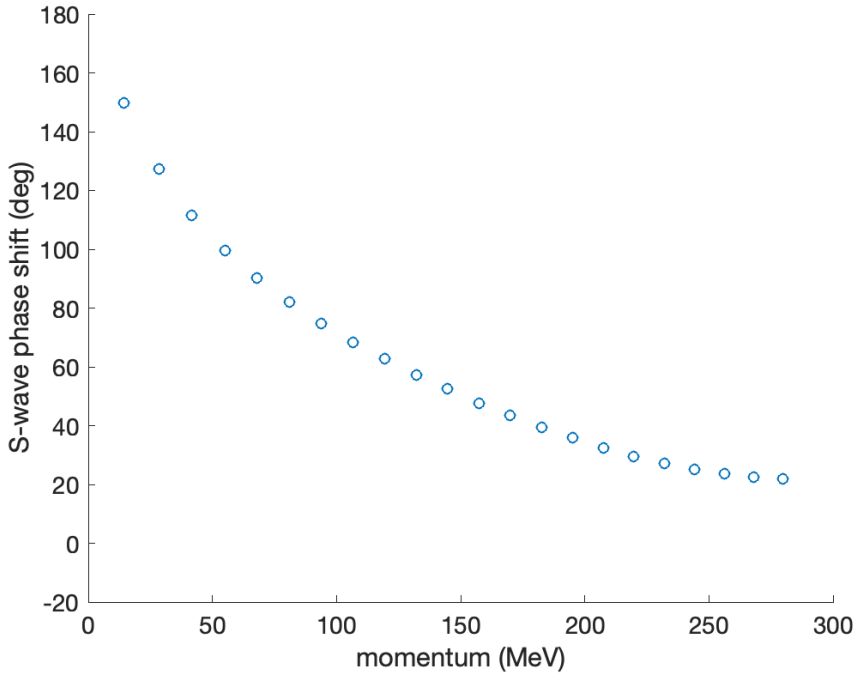
S-wave phase shift (deg)
momentum (MeV)
180
160
140
120
100
80
60
40
20
0
-20
0
50
100
150
200
250
300

Let us write the eigenenergies and eigenfunctions for the two interactions as

$$H_A \left|\psi_{A,n}\right\rangle = \left(K + V_A\right) \left|\psi_{A,n}\right\rangle = E_{A,n} \left|\psi_{A,n}\right\rangle$$
$$H_B \left|\psi_{B,n}\right\rangle = \left(K + V_B\right) \left|\psi_{B,n}\right\rangle = E_{B,n} \left|\psi_{B,n}\right\rangle$$

We would like to compute the eigenenergies of H_A starting from the eigenfunctions of H_B and using first-order perturbation theory.

Not surprisingly, this does not work very well. The interactions V_A and V_B are quite different.

$E_{A,n}$ (MeV)	$\langle\psi_{B,n}\|H_A\|\psi_{B,n}\rangle$ (MeV)
-1.2186	3.0088
0.2196	0.3289
0.8523	1.1275
1.8610	2.2528
3.2279	3.6991
4.9454	5.4786
7.0104	7.5996
9.4208	10.0674
12.1721	12.8799
15.2669	16.0458

Let P be a projection operator that is nonzero only for separation distances r less than R. We define a short-distance unitary operator U such that

$$U : P\,|\psi_A^0\rangle\,/\|P\,|\psi_A^0\rangle\,\| \to P\,|\psi_B^0\rangle\,/\|P\,|\psi_B^0\rangle\,\|$$

There are many possible choices for U. The corresponding action of U on the Hamiltonian is

$$U : H_A \to H'_A = U^\dagger H_A U$$

and the resulting nonlocal interaction is

$$V'_A = H'_A - K = U^\dagger H_A U - K$$

Since they are unitarily equivalent, the phase shifts are exactly the same.

$V_A(r)$

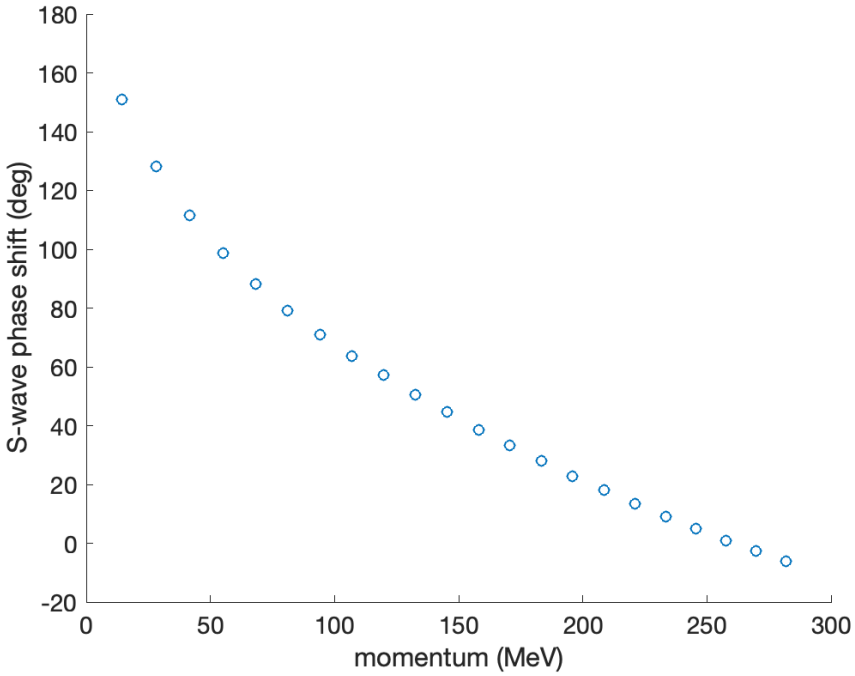

$V'_A(r, r')$

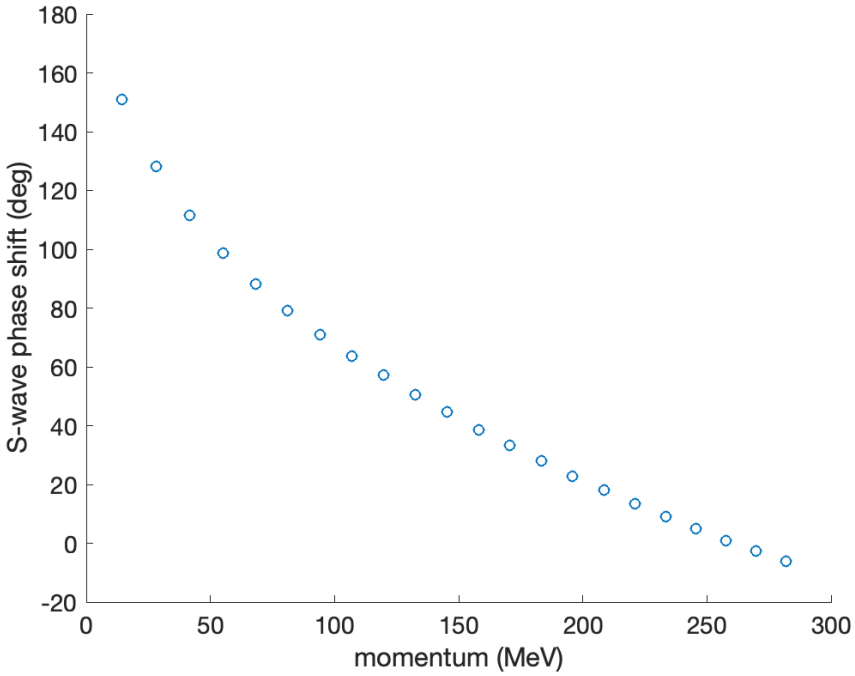

Ground state wave functions

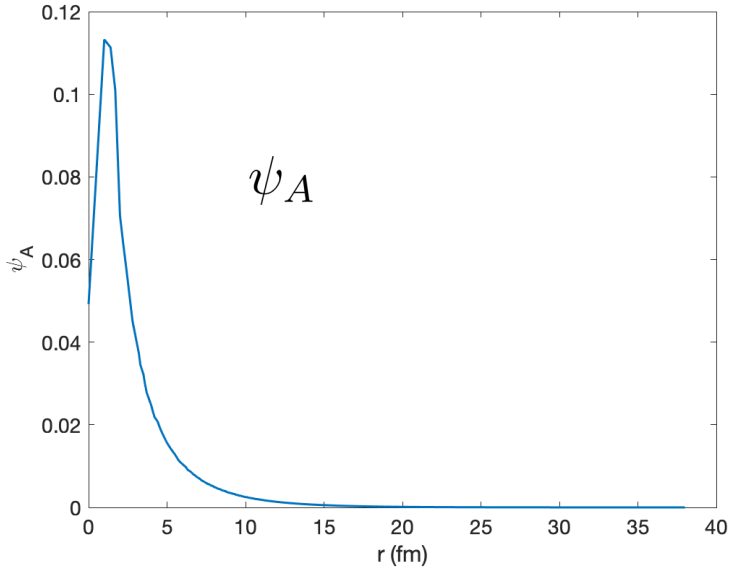

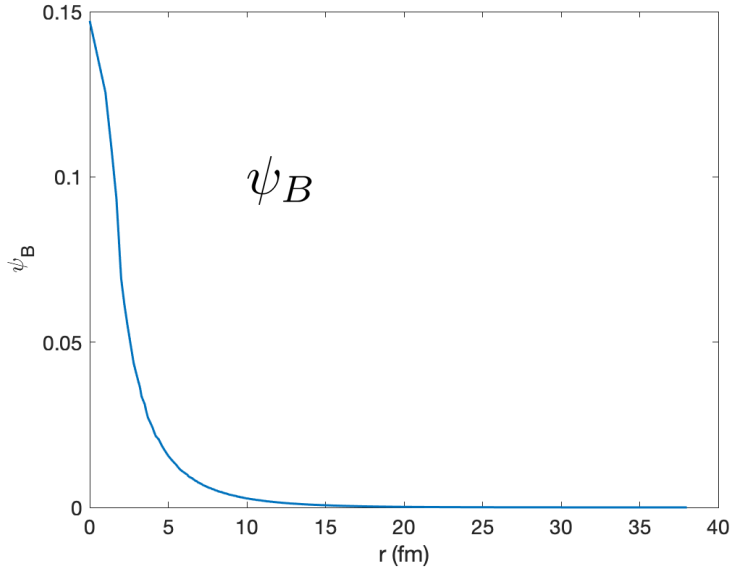

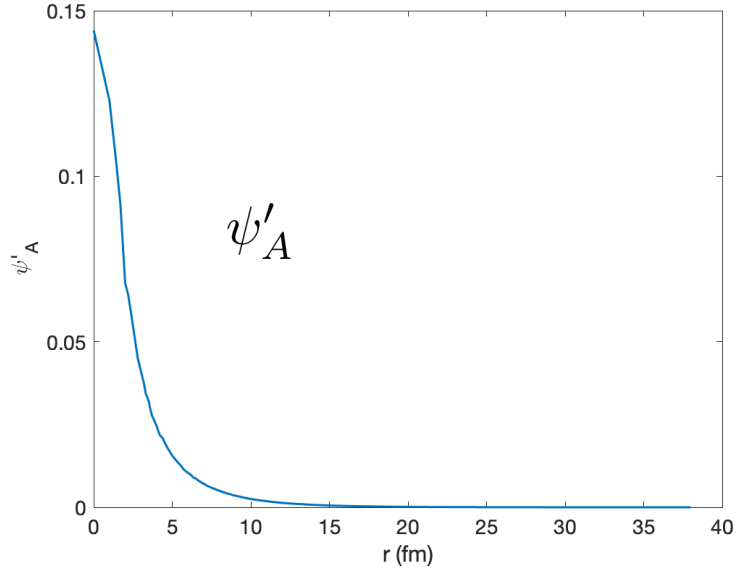

With wave function matching, we can now compute the eigenenergies starting from the eigenfunctions of H_B and using first-order perturbation theory.

$R = 2.6$ fm

$E_{A,n} = E'_{A,n}$ (MeV)	$\langle\psi_{B,n}\|H_A\|\psi_{B,n}\rangle$ (MeV)	$\langle\psi_{B,n}\|H'_A\|\psi_{B,n}\rangle$ (MeV)
-1.2186	3.0088	-1.1597
0.2196	0.3289	0.2212
0.8523	1.1275	0.8577
1.8610	2.2528	1.8719
3.2279	3.6991	3.2477
4.9454	5.4786	4.9798
7.0104	7.5996	7.0680
9.4208	10.0674	9.5137
12.1721	12.8799	12.3163
15.2669	16.0458	15.4840

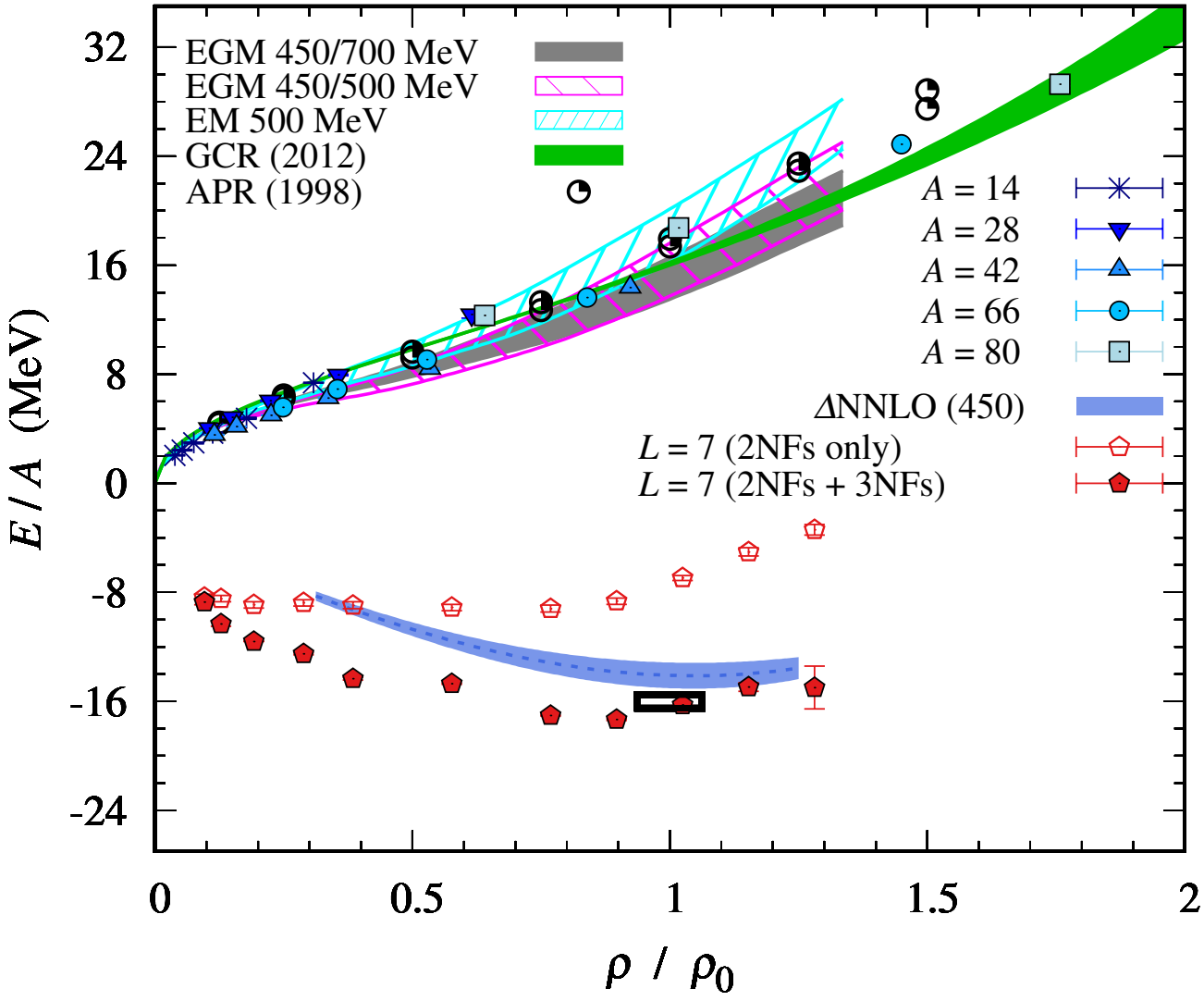
EGM 450/700 MeV
EGM 450/500 MeV
EM 500 MeV
GCR (2012)
APR (1998)
A = 14
A = 28
A = 42
A = 66
A = 80
ΔNNLO (450)
L = 7 (2NFs only)
L = 7 (2NFs + 3NFs)
E / A (MeV)
ρ / ρ0
32
24
16
8
0
-8
-16
-24
0
0.5
1
1.5
2

Chiral lattice results at N3LO using wave function matching

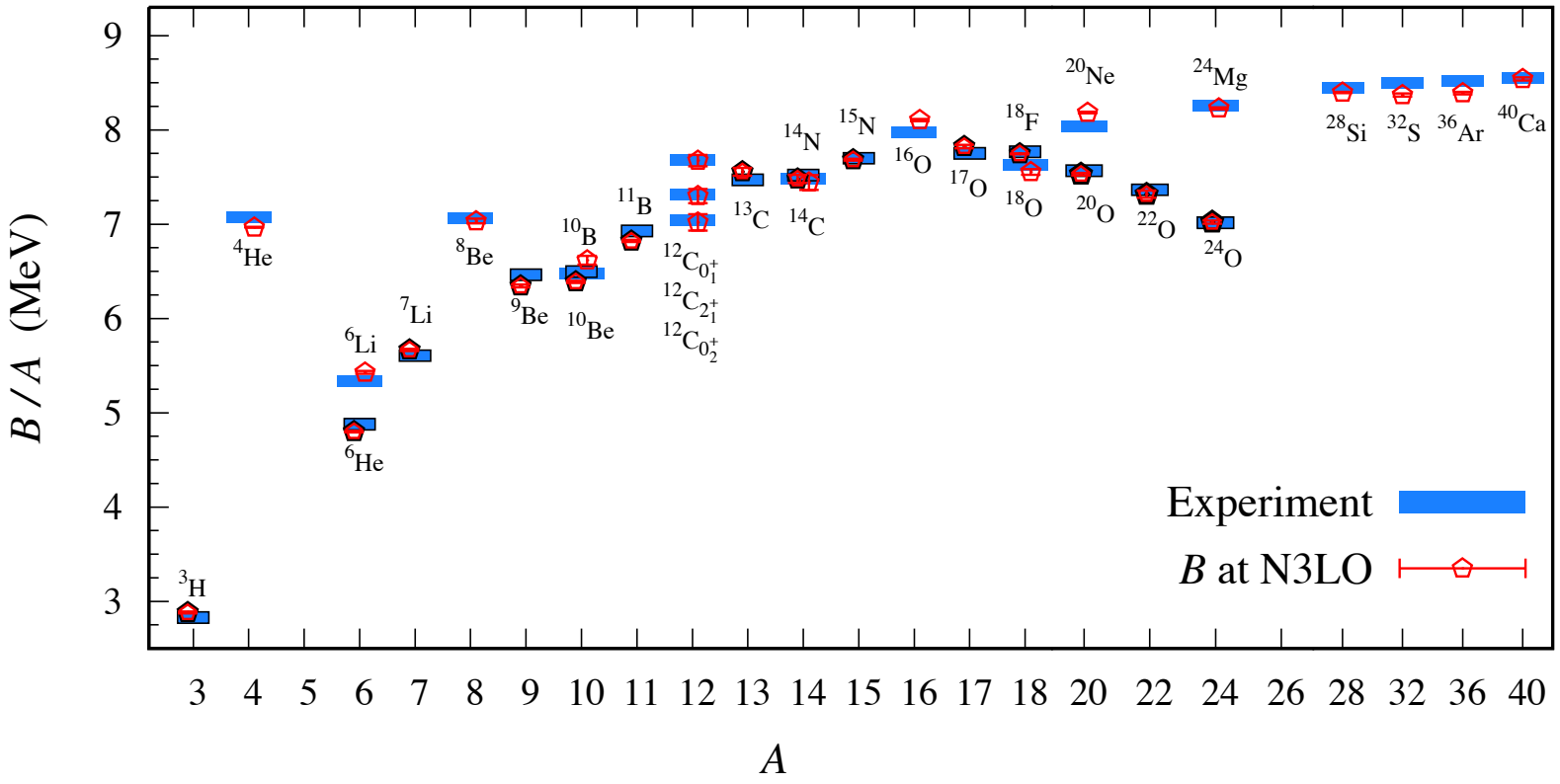

[Work in progress: Elhatisari, Bovermann, et al.]

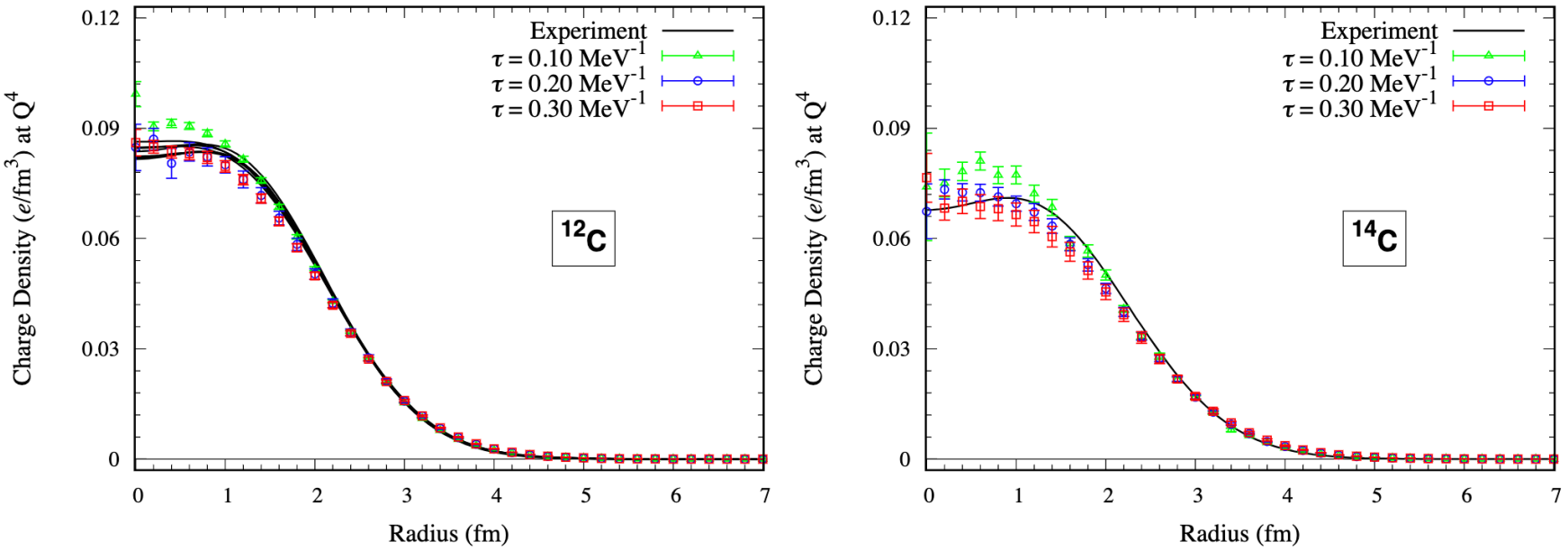

FIG. 4. The plots of the charge densities for the ground states of ^{12}C and ^{14}C at N3LO order in chiral effective field theory compared with the empirical results. The calculated results are shown for different Euclidean time values.

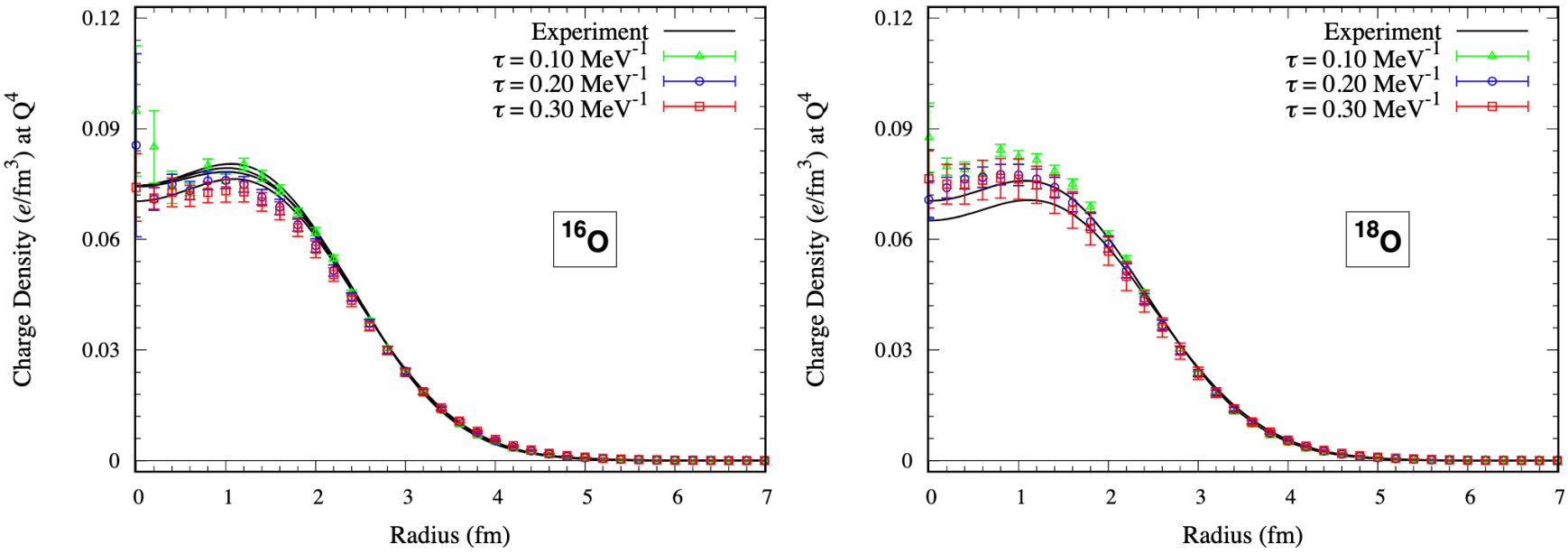

FIG. 5. The plots of the charge densities for the ground states of ^{16}O and ^{18}O at N3LO order in chiral effective field theory compared with the empirical results. The calculated results are shown for different Euclidean time values.

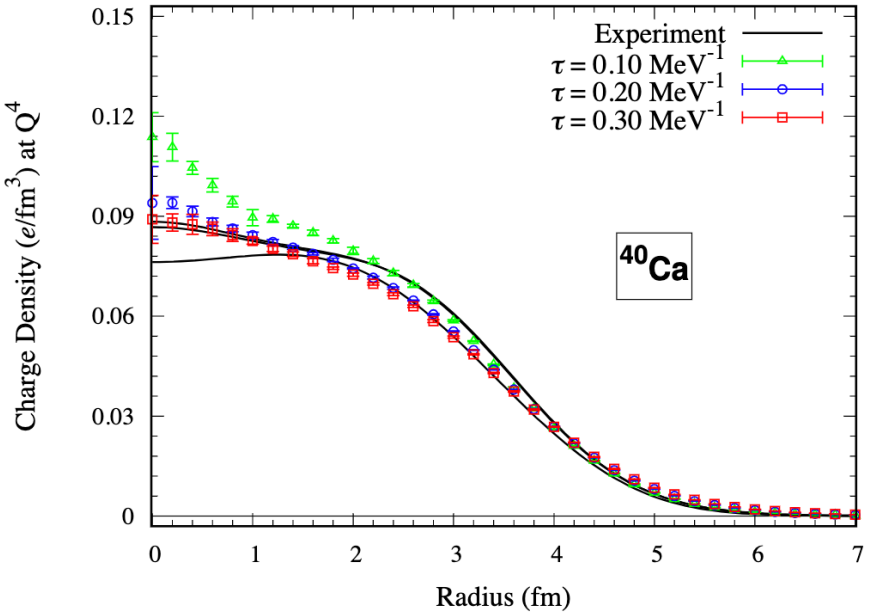

FIG. 6. The plots of the charge density for the ground state of ^{40}Ca at N3LO order in chiral effective field theory compared with the empirical results. The calculated results are shown for different Euclidean time values.

Summary

We started with an introduction to lattice effective field theory. We considered large-N_c arguments that nuclear physics is close to Wigner's SU(4) limit. We then introduced the pinhole algorithm for determining probability distributions of nucleons in position space with full correlations. We then discussed nuclear structure, nuclear thermodynamics, alpha clustering, and the intrinsic structure of the low-lying ^{12}C states. We concluded with a discussion of wave function matching for high-fidelity calculations at N3LO order.